Evapotranspiration in the Amazon: spatial patterns, seasonality and recent trends in observations, reanalysis and CMIP models

Jessica C.A. Baker[1], Luis Garcia-Carreras[2], Manuel Gloor[3], John H. Marsham[1,4], Wolfgang Buermann[5], Humberto R. da Rocha[6], Antonio D. Nobre[7], Alessandro Carioca de Araujo[8] and Dominick V. Spracklen[1]

[1]School of Earth and Environment, University of Leeds, Leeds, UK
[2]School of Earth and Environmental Sciences, University of Manchester, UK
[3]School of Geography, University of Leeds, Leeds, UK
[4]National Centre for Atmospheric Science, Leeds, UK
[5]Institut fuer Geographie, Universitaet Augsburg, D-86135 Augsburg, Germany
[6]Departamento de Ciências Atmosféricas, Instituto de Astronomia, Geofísica e Ciências Atmosféricas, Universidade de São Paulo, Brasil
[7]Earth System Science Center, INPE, Av dos Astronautas, 1758, São José dos Campos, SP Brasil
[8]Empresa Brasileira de Pesquisa Agropecuária (EMBRAPA), Belém-PA, CEP 66095-100, Brasil

Correspondence to: Jessica C.A. Baker (J.C.Baker@Leeds.ac.uk)

Abstract. Water recycled through transpiring forests influences the spatial distribution of precipitation in the Amazon and has been shown to play a role in the initiation of the wet season. However, due to the challenges and costs associated with measuring evapotranspiration (ET) directly, plus the high uncertainty and discrepancies across remote-sensing retrievals of ET, spatial and temporal patterns in this key component of the Amazon hydrological cycle remain poorly understood. In this study, we estimated ET over the Amazon and ten sub-basins using a catchment-balance approach, whereby ET is calculated directly as the balance between precipitation, runoff and change in groundwater storage. We compared our results with ET from remote-sensing datasets, reanalysis, models from the fifth and sixth Coupled Model Intercomparison Projects (CMIP5 and CMIP6), and in-situ flux-tower measurements, to provide a comprehensive overview of current understanding. Catchment-balance analysis revealed a gradient in ET from east to west/southwest across the Amazon basin, a strong seasonal cycle in basin-mean ET controlled by net incoming radiation, and no trend in ET over the past two decades. This approach has a degree of uncertainty, due to errors in each of the terms of the water-budget, therefore we conducted an error analysis to identify the range of likely values. Satellite datasets, reanalysis and climate models all tended to overestimate the magnitude of ET relative to catchment-balance estimates, underestimate seasonal and interannual variability, and show conflicting positive and negative trends. Only two out of six satellite and model datasets analysed reproduced spatial and seasonal variation in Amazon ET, and captured the same controls on ET as indicated by catchment-balance analysis. CMIP5 and CMIP6 ET was inconsistent with catchment-balance estimates over all scales analysed. Overall, the discrepancies between data products and models revealed by our analysis demonstrate a need for more ground-based ET measurements in the Amazon, and to substantially improve model representation of this fundamental component of the Amazon hydrological cycle.

Keywords: transpiration; tropical forest; water-budget; remote sensing; CMIP6

1 Introduction

35   Evapotranspiration (ET) is the transfer of water from the land to the atmosphere through evaporation from soil, open water
and canopy-intercepted rainfall, plus transpiration from plants. More than half of all water that falls as precipitation over land
is recycled back to the atmosphere through ET (Schlesinger and Jasechko, 2014, Good et al., 2015, Jasechko, 2018). This
essential hydrological process affects the partitioning of heat fluxes at the Earth's surface, causing local cooling, while
40   providing moisture for precipitation, thus sustaining the hydrological cycle (Jung et al., 2010, Wang and Dickinson, 2012,
Zhang et al., 2016a). Transpiration is the dominant component of terrestrial ET, and transpiration rates over tropical forests
are among the highest in the world (Zhang et al., 2001, Jasechko et al., 2013, Good et al., 2015, Wei et al., 2017). In the
Amazon, where tropical forest covers approximately 5.5 M km^2, sap flux measurements from a site near Manaus showed the
transpiration contribution to ET increased from 40 % in the wet season up to 95 % in the driest part of the year (Kunert et al.,
45   2017).

Amazon ET is essential for maintaining the regional hydrological cycle and sustaining a climate favourable for tropical
rainforests (Salati and Vose, 1984, Eltahir and Bras, 1994, Eltahir, 1996, Nepstad et al., 2008, van der Ent et al., 2010, Zemp
et al., 2014). Consequently, changes in ET have implications for local and regional climate (Spracklen et al., 2012, Silvério et
50   al., 2015, Spracklen et al., 2018, Baker and Spracklen, 2019) and may impact the stability of the Amazon forest biome (Zemp
et al., 2017a). Deforestation, which has seen a recent upsurge in the region (Barlow et al., 2020), causes reductions in ET,
though the magnitude of the response is still not fully understood. Estimates based on in-situ and remote-sensing data from the
southern Amazon suggest deforestation-driven ET reductions range from 15 to 40% in the dry season (von Randow et al.,
2004, Da Rocha et al., 2009a, Khand et al., 2017, da Silva et al., 2019). Changes in the global climate are also affecting Amazon
55   ET, by increasing atmospheric demand for water vapour, resulting in positive ET trends since the 1980s (Zhang et al., 2015a,
Zhang et al., 2016b, Pan et al., 2020). Over the next century, coupled climate models suggest there may be large reductions in
ET as plants reduce stomatal conductance in response to rising atmospheric CO_2 (Skinner et al., 2017, Kooperman et al., 2018),
leading to changes in the surface energy balance and atmospheric circulation that drive reductions in Amazon rainfall
(Langenbrunner et al., 2019). To assess changes in ET over the Amazon and evaluate climate model credibility, reliable
60   observations of ET are required. However, despite being integral to the health of the Amazon ecosystem, ET over this region
remains a challenging variable to measure and quantify (Pan et al., 2020).

Several early studies used measurements of stable water isotopes to evaluate water recycling over Amazonia, since the isotope
composition of transpired water is distinct from that of evaporated water (Salati et al., 1979, Victoria et al., 1991, Martinelli et
65   al., 1996, Moreira et al., 1997). Such work first highlighted the predominance of transpiration over Amazonia, relative to
continental areas with lower forest cover, such as Europe (Salati et al., 1979, Gat and Matsui, 1991). More recently, studies
based on satellite retrievals of hydrogen isotopes in tropospheric water vapour have suggested that transpiration could be key

in triggering convection during the Amazon dry-to-wet season transition (Wright et al., 2017), and that ET reductions in the 2005 drought caused a delay in wet-season onset in the following year (Shi et al., 2019). However, while isotopes can help to

70   partition ET into its respective components, they cannot provide information about the absolute magnitude of the ET flux, and thus other methods are required to quantify ET.

Amazon ET can be quantified using a catchment-balance approach, whereby ET is approximated as the difference between precipitation and runoff. Estimates of annual mean Amazon ET using this method range from 992 to 1905 mm yr^{-1} (mean±σ

75   = 1421±254 mm yr-1; Marengo, 2006 and references therein), though part of this uncertainty is due to differences in the definition of Amazon basin extent. Historically, water budget approaches have assumed that groundwater storage does not change over time, though more recent studies have been able to also account for changes in groundwater using terrestrial water storage anomalies measured by the Gravity Recovery and Climate Experiment (GRACE) satellites (i.e. Swann and Koven, 2017, Maeda et al., 2017, Sun et al., 2019). Swann and Koven (2017) estimated annual mean Amazon ET to be 1058 mm yr^{-}

80   ^{1}, which is towards the lower end of previous estimates. Constraining Amazon ET in this way is useful, though a whole-basin-scale analysis by definition does not capture spatial variation in Amazon ET. Maeda et al. (2017) used a water balance approach to estimate ET in five Amazon sub-basins, and found values ranging from 986 mm yr^{-1} in the Solimões basin in the western Amazon, to 1497 mm yr^{-1} in the northern Negro basin. However, even this sub-basin-scale analysis is likely to mask finer-scale spatial heterogeneities in ET.

85

Direct, site-level measurements of ET can be obtained from eddy-covariance (EC) flux towers. During the 1990s, a network of towers was established in Brazil as part of the Large-Scale Biosphere-Atmosphere Experiment in Amazonia (LBA) research programme (see Keller et al., 2009, and references therein). ET measurements from these towers have provided valuable insights into the drivers of variability in Amazon ET and how ET varies over different temporal scales (da Rocha et al., 2004,

90   Hasler and Avissar, 2007, Fisher et al., 2009, Restrepo-Coupe et al., 2013, Christoffersen et al., 2014). EC data have shown that surface net radiation is the primary control on seasonal Amazon ET over wet areas of the Amazon (precipitation above 1900 mm), while variation in water availability governs ET in the seasonally-dry tropical forests in the south and southeast Amazon, towards the boundary with the Cerrado biome (da Rocha et al., 2009b, Costa et al., 2010). Despite these advances in understanding, it should be noted that EC measurements have an inherent degree of uncertainty, as measured turbulent heat

95   fluxes do not sum to the total measured available energy (i.e. the energy balance closure problem, Wilson et al., 2002, Foken, 2008). Tropical forest LBA tower sites underestimated the total energy flux by 20–30 % (Fisher et al., 2009), indicating that part of the ET flux might have been missed. A study in western Europe also suggested that flux towers may underestimate ET over forests compared to ET from lysimeters and water-balance methods (Teuling, 2018). Variation in energy closure between flux tower sites also makes it difficult to make direct comparisons between absolute ET values measured in different locations,

100   presenting a further challenge (da Rocha et al., 2009b). Finally, the spatial distribution of flux towers in South America is uneven, with no EC ET measurements currently available over large areas of the western and northern Amazon (see Fig. 1).

Given the relatively high costs associated with setting up and running flux towers, and the inaccessibility of much of the Amazon basin, it is desirable to find alternative methods of monitoring ET over this region of remote tropical forest and elsewhere.

105

Over the past few decades, ET products derived from Earth observation satellites have become available (e.g. Mu et al., 2007, Zhang et al., 2010, Miralles et al., 2011, Mu et al., 2011, Martens et al., 2017). These products offer ET estimates over previously unmonitored regions, such as the western Amazon, and therefore have potential to further our understanding of the controls and drivers of the Amazon hydrological cycle. Satellite-based ET products provide spatially and temporally

110 homogeneous information at scales that are well suited for climate model evaluation. However, it is important to note that these products are not direct measures of ET, but rather ET is estimated from variables that satellites do measure (essentially radiation), other satellite retrievals (e.g. LAI) and, crucially, model-derived inputs. Thus, although often referred to as 'observational datasets', it is more accurate to consider satellite ET products as physically-constrained land-surface models. Global-scale ET product comparisons have been conducted before, for example as part of the WACMOS-ET (WAter Cycle

115 Multi-mission Observation Strategy – EvapoTranspiration) project (Michel et al., 2016, Miralles et al., 2016), and a more recent detailed evaluation that included multiple remote-sensing datasets and 14 land-surface models (Pan et al., 2020). While these studies made some comparisons between products over the Amazon, they did not include any 'ground-truth' validation data over South America. Further work has evaluated individual products over the Amazon at different spatial scales (e.g. Ruhoff et al., 2013, de Oliveira et al., 2017, Maeda et al., 2017, Swann and Koven, 2017, Sörensson and Ruscica, 2018, Paca

120 et al., 2019), though a detailed analysis of spatial and temporal variation in remote-sensing ET products, evaluated against ET from catchment-balance analysis and flux towers, is currently lacking.

Finally, representation of Amazon ET in coupled climate models is still underdeveloped. A synthesis of observations, reanalysis and land-surface model output showed Amazon ET tended to be overestimated at the annual scale in 14 models

125 from the fifth Coupled Model Inter-comparison Project (CMIP5), but underestimated from June to August (Mueller and Seneviratne, 2014). More recently it was observed that 28 out of 40 CMIP5 models analysed misrepresented the controls on ET over the Amazon, with implications for future precipitation projections in the region (Baker et al., in review at NCC). Other assessments of CMIP5 models over the Amazon have found that choice of reference ET dataset can have a large impact on model performance metrics (Schwalm et al., 2013, Baker et al., in review at Journal of Hydrometeorology). With output from

130 the sixth generation of CMIP models now available (Eyring et al., 2016), there is a need for clarity over the reliability of Amazon ET products that are widely used for model evaluation.

The aim of this study was to summarise the current 'state-of-the-science' for Amazon ET in an attempt to determine what aspects of Amazon ET are well understood, identify areas of remaining uncertainty, and provide a benchmark to evaluate the

135 latest generation of coupled climate models. Given the challenges associated with estimating ET, we collated data from a

variety of sources, expanding earlier studies by including 'direct' estimates of ET from catchment-balance analysis and flux towers in our validation. Our work extends earlier studies by deriving ET estimates for ten Amazon sub-basins, permitting an assessment of controls on spatial variation in ET. Our results highlight substantial differences between ET products, while our catchment-balance analysis provides new insights on the spatial and temporal patterns of ET variability over the Amazon
140   basin.

2 Data and Methods

To capture a complete spectrum of ET estimates over the Amazon, we combined data from catchment-balance analysis, flux towers, remote-sensing products, reanalysis and coupled climate models. The origins of these datasets are described in the sections that follow.

145   **2.1 Catchment-balance ET**

Catchment-balance ET provides the closest approximation to a direct ET 'measurement' over large spatial scales in this study. In this approach, ET is calculated as the difference between terms in the water-budget equation that can be measured (within a margin of error), following Eq. (1):

$$\text{ET} = P - R - \frac{dS}{dt} \qquad (1)$$

150   where P is area-weighted, catchment-mean precipitation, R is river runoff from the basin, and $\frac{dS}{dt}$ is the area-weighted, basin-mean change in terrestrial water storage (S) over the basin with respect to time (t), all in units of mm month[-1]. Catchment-balance ET was calculated, first as the simple difference between precipitation and runoff (climatological basin means only), and then using the more sophisticated approach that accounts for temporal variation in groundwater storage (Rodell et al., 2011, Long et al., 2014, Swann and Koven, 2017, Maeda et al., 2017, Sun et al., 2019).

155

The catchment-balance approach was used to estimate climatological annual mean ET for the Amazon basin and ten sub-catchments: the Solimões, Japura, Negro, Branco, Jari, Purus, Madeira, Aripuanã, Tapajos and Xingu catchments (Fig. 1). Temporal variation in catchment ET was analysed for the Amazon basin only. Basin domains were constructed by aggregating sub-basin shapefiles that had previously been identified using a digital elevation model (Seyler et al., 2009), making sure to
160   include all sub-basins upstream of the relevant river station.

Precipitation data came from the 0.05° x 0.05° Climate Hazards Group InfraRed Precipitation with Station (CHIRPS) dataset, which combines data from satellites and rain gauges (Funk et al., 2015). CHIRPS has been validated against rain-gauge data from northeast Brazil, including four Amazon stations, and found to have mean bias and absolute error values of –3.6% and
165   28.4 mm month[-1], respectively (Paredes-Trejo et al., 2017).

Monthly-mean river flow data were obtained from the Agência Nacional de Águas (ANA) database in Brazil (HidroWeb, 2018). To obtain runoff in mm month^{-1}, volumetric flow rates (m^3 s^{-1}) were divided by the catchment area (m^2), scaled to the monthly timestep by multiplying by the number of seconds in each month and multiplied by 1000 to convert to mm. To

170 estimate 'whole' Amazon ET, we used runoff measured at Óbidos, which drains approximately 77 % (Callède et al., 2008) of the Amazon basin (Fig 1). For the Tapajos catchment, runoff from Itaituba, was gap-filled based on linear regression with data from the Buburé station, which is approximately 70 km upstream (R^2=0.77, 15 data points in total). Details of the gauge stations used for the other basin river records are provided in Table S1.

175 Terrestrial water storage data were derived from the 0.5° x 0.5° Jet Propulsion Laboratory (JPL) RL06M Version 2.0 GRACE Mascon Solution, with Coastline Resolution Improvement (CRI) filtering and land-grid scaling factors (derived from the Community Land Model, CLM) applied (Watkins et al., 2015, Wiese et al., 2016, Wiese et al., 2018). This dataset, which has been processed to minimise measurement errors and optimise the signal-to-noise ratio, represents a new generation of GRACE solutions that do not require empirical post-processing to remove correlated errors, and are thus considered more rigorous than

180 the previous GRACE land water storage estimates based on spherical-harmonic solutions (Wiese et al., 2016).

To determine the change in water storage, $\frac{dS}{dt}$, in units of mm month^{-1}, we calculated the difference between consecutive GRACE measurements for each grid cell, divided by the time between measurements, as shown in Eq. (2):

$$\frac{dS}{dt} = (S_{[n]} - S_{[n-1]})/dt \qquad (2)$$

185 where S represents the land water storage anomaly in mm, n is the measurement number and dt is the time between measurements $[n]$ and $[n–1]$ in months. Following this, we calculated the area-weighted, basin-mean $\frac{dS}{dt}$ for each catchment. Finally, to account for the uneven temporal sampling of GRACE data, we used a linear spline to interpolate $\frac{dS}{dt}$ values to the same temporal grid as the precipitation and runoff data, i.e. one value per month for the period May 2002 to December 2019.

190 Previous work has shown that GRACE is less sensitive at lower latitudes than at higher latitudes, and may only be capable of detecting monthly changes in groundwater storage over regions larger than 200,000 km^2, or seasonal changes over areas greater than 184,00 km^2 (Rodell and Famiglietti, 1999). Three of the basins included in this analysis have areas smaller than these thresholds, namely Jari (49,000 km^2), Branco (131,000 km^2) and Aripuanã (138,000 km^2, Table S1). However, we only computed climatological means over these basins, and the catchment-balance ET estimates were in excellent agreement with

195 ET calculated as the difference between precipitation and runoff (r=0.997, p<0.001, Fig. S1). Therefore, we have confidence that our results for these basins were not biased by the inclusion of GRACE in the calculations.

For the Amazon basin only, we calculated catchment-balance ET at the monthly timescale. We estimated the relative uncertainty of our ET estimates (υ_{ET})υ_{ET}) by propagating errors in each of the terms of the water budget equation (Rodell et

200   al., 2011), following Eq. (3):

$$\upsilon_{ET} = \frac{\sqrt{\sigma_P{}^2 + \sigma_R{}^2 + \sigma_{\frac{dS}{dt}}{}^2}}{ET} \quad (3)$$

where σ_P, σ_R and $\sigma_{\frac{dS}{dt}}$ respectively represent the absolute uncertainties in P, R and $\frac{dS}{dt}$. Errors in precipitation were estimated as the random error (σ_{P_random}) plus the systematic error (σ_{P_bias}), combined in quadrature. Random errors were calculated following Eq. (4), from Huffman (1997):

205

$$\sigma_{P\_random} = \bar{r} \left[\frac{H - p}{pN} \right]^{\frac{1}{2}} \quad (4)$$

where $\bar{r}$ is the climatological mean precipitation over the basin, H is a constant (1.5), p is the frequency of non-zero rainfall and N is the number of independent precipitation samples (defined as the number of Amazon pixels with finite P measurements in each month). For σ_{P_bias}, we used the value of –3.6 % estimated for CHIRPS from a validation analysis based on data from 21 meteorological stations in northeast Brazil (Table 4 in Paredes-Trejo et al., 2017). σ_R was estimated as 5% of monthly river

210   flow (Dingman, 2015). Uncertainty in groundwater storage was quantified by combining GRACE measurement errors and leakage errors (residual errors after filtering and rescaling) in quadrature. For these, we used Amazon-specific values from the literature (6.1 and 0.9 mm for measurement and leakage errors, respectively) that had been calculated after CRI filtering and CLM scaling factors had been applied (Table 1 in Wiese et al., 2016). Finally, since $\frac{dS}{dt}$ values were calculated using data from two consecutive months, groundwater error values were multiplied by $\sqrt{2}$ to obtain $\sigma_{\frac{dS}{dt}}$ (e.g. Maeda et al., 2017). We

215   calculated a mean υ_{ET} value of 16.1 % (standard deviation=9.2 %) for Amazon catchment-balance ET (Fig. S2). At the monthly timescale, the $\frac{dS}{dt}$ and precipitation terms were found to be the dominant sources of uncertainty ($\sigma_{\frac{dS}{dt}}$=8.7 mm, σ_P=6.8 mm), followed by runoff (σ_R=4.9 mm, Table S2). Seasonal and interannual time series of precipitation, runoff, $\frac{dS}{dt}$ and ET, and their associated errors, are shown in Figures S3 and S4. Due to small interannual variation in $\frac{dS}{dt}$ (Fig. S4), climatological estimates of ET calculated with and without water storage estimates were similar (Figs. 1 & 2). Data from August 2017 to

220   June 2018 were removed due to anomalously low and possibly unreliable $\frac{dS}{dt}$ data over this period (Fig. S4c).

2.2 Flux tower ET

To provide a ground-truth perspective, we used the 1999–2006 quality-controlled (QAQC), monthly flux tower ET observations from six flux towers in the LBA BrasilFlux database (Restrepo-Coupe et al., 2013, Saleska et al., 2013). These data have been processed to remove unreliable or low-quality measurements, and can be downloaded from the LBA web page:

225   https://daac.ornl.gov/LBA/guides/CD32_Brazil_Flux_Network.html. We selected towers situated over land-cover types that

were representative of the surrounding area, including towers in forest, savanna and floodplain sites, but excluding towers in sites where pasture was the dominant regional land use (see Table S3). The site locations are shown in Figure 1. We calculated ET in units of mm month^{-1} (kg m^{-2} month^{-1}) using Eq. (5):

$$ET = (LE/\lambda) \qquad (5)$$

230 where LE is the monthly mean tower measurement of latent heat flux (W m^{-2} = J s^{-1} m^{-2}), scaled to J month^{-1} m^{-2}, and λ is the latent heat of vaporization at 20°C (2.453 x 10^{6} J kg^{-1}).

In addition to the QAQC LBA data, we used a unique 19-year record (1999–2017) for the K34 flux-tower site (2.6°S, 60.2°W) near to Manaus, Brazil. Unlike the other tower sites, where data were only available for a few years (Table S3), this extended
235 record could be used to derive a robust seasonal cycle in ET. Half-hourly data were averaged and scaled to obtain monthly means. To test the sensitivity of our results to missing data, we applied thresholds for the minimum number of hours or days required to calculate a mean value each month. Seasonal results were found to be relatively insensitive to minimum data requirement thresholds, thus we decided to include all monthly ET measurements in our analysis (Table S4).
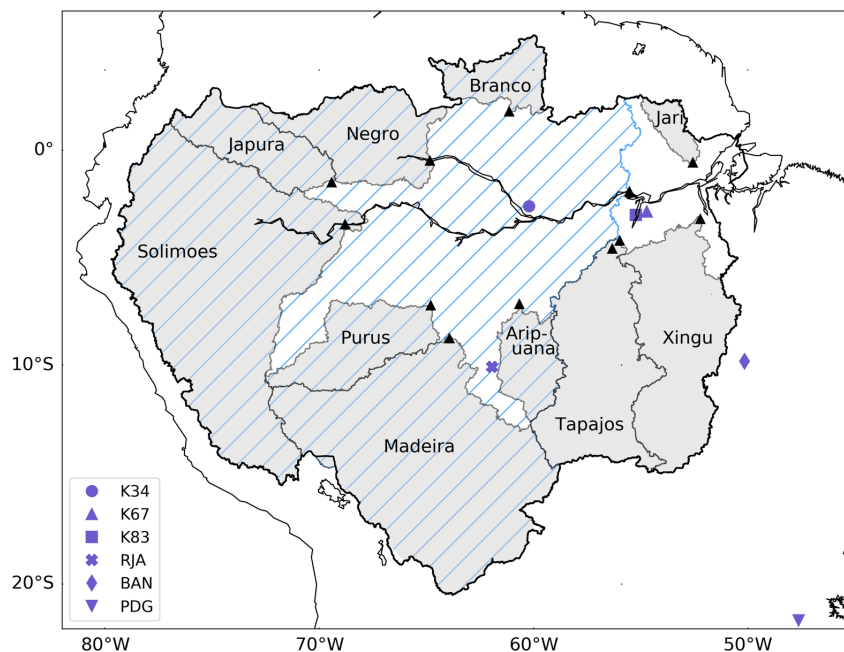
240

Figure 1 – Locations of river catchments and in-situ data. Map showing the locations of the Amazon sub-basins (grey polygons) and the respective river-gauge stations (black triangles) used to estimate catchment-balance ET. Note that two stations in the Tapajos basin were used (see Methods). Blue hatching indicates the area drained by the Óbidos measurement station, which is used to represent 'whole' Amazon ET. The locations of the LBA flux towers used in the study are also shown

245 (purple markers, see Table S3 for site information). The markers for K67 and K83 have been offset by 0.25° in longitude and
latitude, respectively, to improve visibility.

2. 3 Satellite and reanalysis ET

Three global, satellite-derived ET products and one reanalysis dataset were included in this study. The Moderate Resolution
Imaging Spectroradiometer (MODIS) MOD16A2 ET product (Mu et al., 2011, Mu et al., 2013) was downloaded at 500-m
250 resolution from the NASA Earth Data web page (https://earthdata.nasa.gov) for the period 2001–2019. The MODIS ET
algorithm is based on the Penman-Monteith equation (Monteith, 1965), which uses temperature, wind speed, relative humidity
and radiation data to approximate net ET, but modified by scaling canopy conductance by leaf area index. We also obtained
ET estimates from the 8-km Process-based Land Surface ET/Heat Fluxes algorithm (P-LSH) product provided by the
Numerical Terradynamic Simulation Group at the University of Montana (Zhang et al., 2010, Zhang et al., 2015a) for the
255 period 1982–2013. This ET product is also based on the Penman-Monteith equation but uses an algorithm that incorporates
remote-sensing NDVI data to estimate canopy conductance. Additionally, ET were retrieved from the satellite-constrained
Global Land Evaporation Amsterdam Model (GLEAM) v3.3b dataset (Miralles et al., 2011, Martens et al., 2017) at 0.25° x
0.25°. This version of GLEAM is based on satellite data only, and available for the period 2003–2018. GLEAM is based on
the Priestley-Taylor framework (Priestley and Taylor, 1972), which uses temperature and radiation to estimate potential ET
260 (PET), together with a hydrological model to convert PET to actual ET. Finally, 0.25° x 0.25° ET data were retrieved for the
period 1979–2019 from the European Centre for Medium-Range Weather Forecasts ERA5 reanalysis, which incorporates
observations into a model to provide a numerical description of historical climate (Hersbach et al., 2018). Since ET is not
among the many observations that are assimilated in the reanalysis, ERA5 ET is independent from the other ET datasets
analysed in this study. To permit a meaningful comparison between datasets, all satellite and reanalysis ET products were re-
265 gridded to 0.25°, analysed at the monthly timescale, and averaged over the common time period of 2003–2013 for those
analyses based on temporal means. A summary of the equations and datasets used to derive the satellite ET products is
presented in Table 1.

2.4 ET from coupled climate models

We obtained historical simulations of ET from models participating in CMIP5 and CMIP6 for the periods 1994–2004 and
270 2001–2014, respectively. We selected models that also provided precipitation, surface shortwave radiation and leaf area index
(LAI) output, in order to investigate model processes controlling ET. In total, we used data from 13 CMIP5 models, and 10
CMIP6 models (Tables S5 and S6). Output was downloaded at monthly resolution from the Centre for Environmental Data
Analysis archives (http://archive.ceda.ac.uk), accessed via the JASMIN supercomputer. Where available, multiple realisations
were used to derive an ensemble mean for each model, else a single run was used. For basin-scale ET estimates, annual and
275 seasonal climatological means were calculated for each model separately, using native-resolution data, and then subsequently
averaged across models. For CMIP5, climatologies were computed using data from 1994–2004 (most recent 11 years of

available data), while CMIP6 climatologies were estimated using the same period as for observations (i.e. 2003–2013). To visualise spatial variation in ET over the Amazon and make comparisons with site-level ET measurements, multi-model ensemble means were also computed for CMIP5 and CMIP6. To do this, we re-gridded ET from each model to 1° x 1° and 280 then calculated the ensemble mean across all models.

Table 1 – Details of the evapotranspiration (ET) datasets analysed in this study.

ET data	Product(s)	Core equation	Input datasets	References
Catchment-balance	Computed in this study	ET = P–R or ET = P–R– dS/dt	– CHIRPS P – R from ANA – GRACE S	Funk et al. (2015) HidroWeb (2018) Wiese et al. (2018)
Satellite	MODIS MOD16A2	Penman-Monteith (Monteith, 1965)	– MODIS land cover (MOD12Q1) – MODIS FPAR/LAI (MOD15A2) – MODIS albedo (MOD43C1) – GMAO v 4.0.0 reanalysis meteorology data	Mu et al. (2007) Mu et al. (2011)
	P-LSH	Penman-Monteith (Monteith, 1965)	– AVHRR GIMMS NDVI – NCEP/NCAR reanalysis meteorology data – NASA GEWEX radiation – FLUXNET tower data to parameterise canopy conductance model	Zhang et al. (2010) Zhang et al. (2015a)
	GLEAM v3.3b	Priestley-Taylor (Priestley and Taylor, 1972)	– CERES L3 SYN1DEG Ed4A radiation – AIRS L3 RetStd v6.0 air temperature – MSWEP v2.2 precipitation – GLOBSNOW L3Av2 & NSIDC v01 snow water equivalent – LPRM vegetation optical depth – ESA-CCI 4.5 soil moisture – MEaSUREs VCF5KYR_001 vegetation fractions	Martens et al. (2017)
Reanalysis	ERA5	Global model	A full list of input datasets is provided here: https://confluence.ecmwf.int/display/CKB/ERA5%3A+data+documentation#ERA5:datadocumentation-Observations	Hersbach et al. (2018)
Climate model	CMIP5	Global model	13 Earth System Models (Table S5)	Taylor et al. (2012)
	CMIP6	Global model	10 Earth System Models (Table S6)	Eyring et al. (2016)

2.5 Dataset inter-comparison

We compared differences in ET magnitude, spatial variation, seasonality and trends over the past two decades, identifying where estimates were in good agreement and where inconsistencies occurred. For annual comparisons, we computed climatological means over the Amazon basin (area drained by Óbidos, Fig. 2) and its sub-catchments (Fig. 3), using an area-weighted averaging approach. We examined how well each ET product was able to capture spatial variation in Amazon ET, through comparisons with catchment-balance ET estimates and flux-tower measurements, and from correlating basin-scale annual means with catchment-balance ET (Table S7). ET products were also evaluated at the seasonal timescale over the Amazon catchment and at the K34 flux tower site (Fig. 1). For comparisons between flux tower and gridded ET data, we selected data from the single grid cell containing the tower. Finally, we analysed linear trends in ET over the past two decades using ordinary least squares regression. Data were analysed over the time period common to all datasets (2003–2013), and across all years with available data for each dataset. Gaps in the interannual catchment-balance ET time series were filled with the climatological mean value prior to calculating linear trends.

2.6 Investigating controls on Amazon ET

To better understand differences between ET products, we analysed relationships with potential drivers of ET, including precipitation, surface radiation and LAI. In addition to comparing area-weighted catchment means and seasonal cycles over the Amazon, we analysed the response of ET to spatial variation in its potential drivers at the grid-cell level, following a similar approach to Ahlström et al. (2017). This enabled us to better understand non-linear relationships between ET and its controlling variables. Mean annual ET values from all Amazon grid cells were binned by annual precipitation, radiation and LAI using bin widths of 100 mm, 5 W m^{-2} and 0.2 m^2 m^{-2} respectively. Bins with fewer than five data points were excluded from the analysis. ET from satellite products, reanalysis and climate models were compared against data from corresponding sources. For ERA5, we used the 'high vegetation' LAI field since the Amazon is predominantly covered with tropical forest, though repeating the analysis with 'low vegetation' LAI made little difference to the results. Thus, satellite ET was compared with precipitation from CHIRPS, radiation from CLARA-A1 (Karlsson et al., 2013) and LAI from the MODIS MOD15A2H product (Myneni et al., 2015), each re-gridded to 0.25° x 0.25°, while reanalysis and model ET were compared with reanalysis and model variables, respectively. Note that the satellite-based MODIS ET product incorporates MODIS LAI (Table 1), and thus these datasets are not fully independent from one another. All data were from 2003–2013, with the exception of CMIP5, which covered 1994–2004. For the K34 tower site, ET was compared against precipitation and radiation data only. Half-hourly measurements of precipitation and incoming radiation from the tower site were averaged and scaled to monthly resolution, following the same procedures as applied to the ET data. Due to missing data in several years, climatological means and seasonal cycles were calculated using all data from 1999–2017.

3 Results and Discussion

3.1 Comparing estimates of annual ET over the Amazon

Climatological annual Amazon ET estimates from water-balance approaches, satellite-based products, reanalysis and two coupled-model ensembles are presented in Figure 2. ET from catchment-balance was the lowest of all estimates (mean ± standard deviation = 1083±37 mm year^{-1} for 2003–2013, Fig. 2, Table S7), which, given uncertainties, is indistinguishable from the value obtained from differencing precipitation and runoff (1102±53 mm year^{-1}). This confirms that the GRACE-observed changes in groundwater storage are relatively small over decadal timescales. Our mean annual catchment-balance ET estimate for the Amazon was very similar to that from a previous catchment-balance study (1058 mm yr^{-1}), calculated over the same drainage region (drained by Óbidos) but based on different precipitation data and an alternative GRACE solution (Swann and Koven, 2017), suggesting the approach is relatively robust. The area drained by Óbidos excludes the far eastern Amazon, which our spatial catchment-balance analysis revealed to have the highest annual ET across the basin, decreasing towards the west and south (Fig. 3a, b). This may explain why our catchment-balance annual Amazon ET value was towards the lower end of previous estimates (Marengo, 2006).
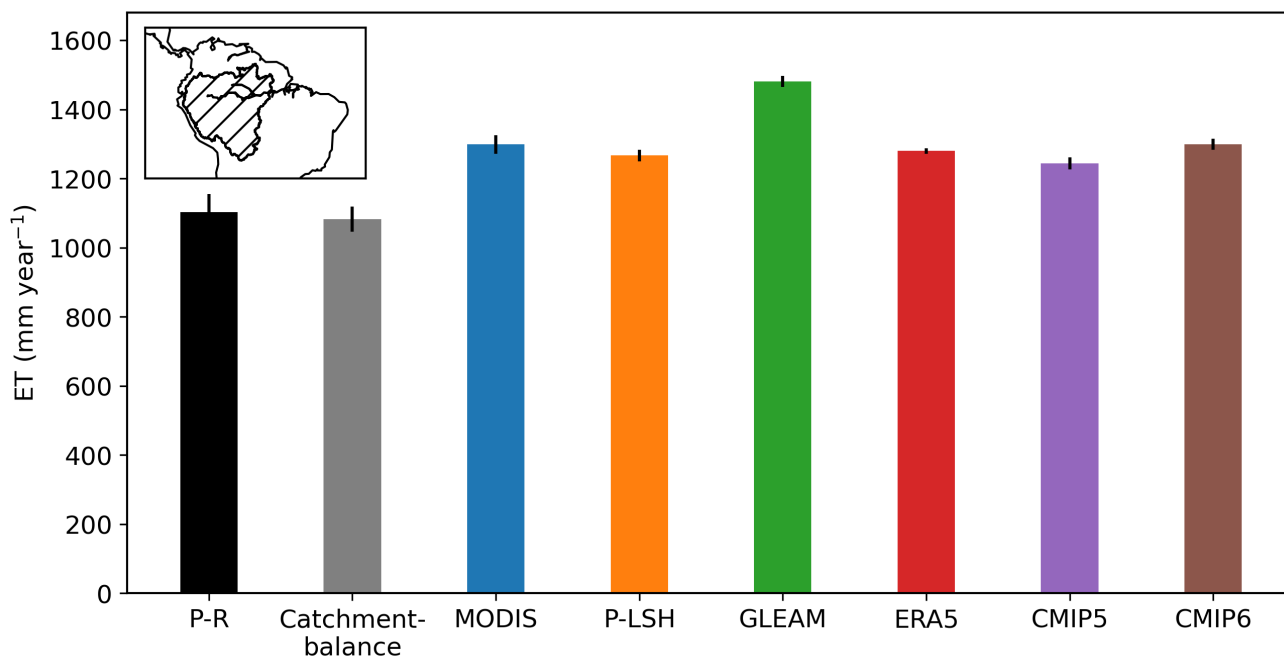
Figure 2 – Comparison of annual Amazon evapotranspiration (ET) estimates. Climatological mean Amazon ET estimated from water-balance approaches (precipitation–runoff, P–R; catchment-balance), satellites (MODIS, P-LSH, GLEAM), ERA5 reanalysis, and climate models (CMIP5 and CMIP6). Data are from 2003 to 2013, with the exception of CMIP5, where the data are from 1994–2004. Error bars represent the interannual standard deviation for each dataset. For CMIP5 and CMIP6 the error bars represent the average standard deviation across all models.

335   Annual Amazon ET from satellites, reanalysis and coupled models was 15–37 % higher than catchment-balance ET, with GLEAM showing the largest bias (Fig. 2). With the exception of GLEAM, annual ET values from satellites, reanalysis and coupled models were remarkably similar to one another (within 50 mm, or <4%), with a mean bias of 18 % (relative to catchment-balance ET). This substantial and consistent overestimation of annual Amazon ET across data products and coupled models highlights that even basic features of the Amazon hydrological cycle are still not well characterised.

340
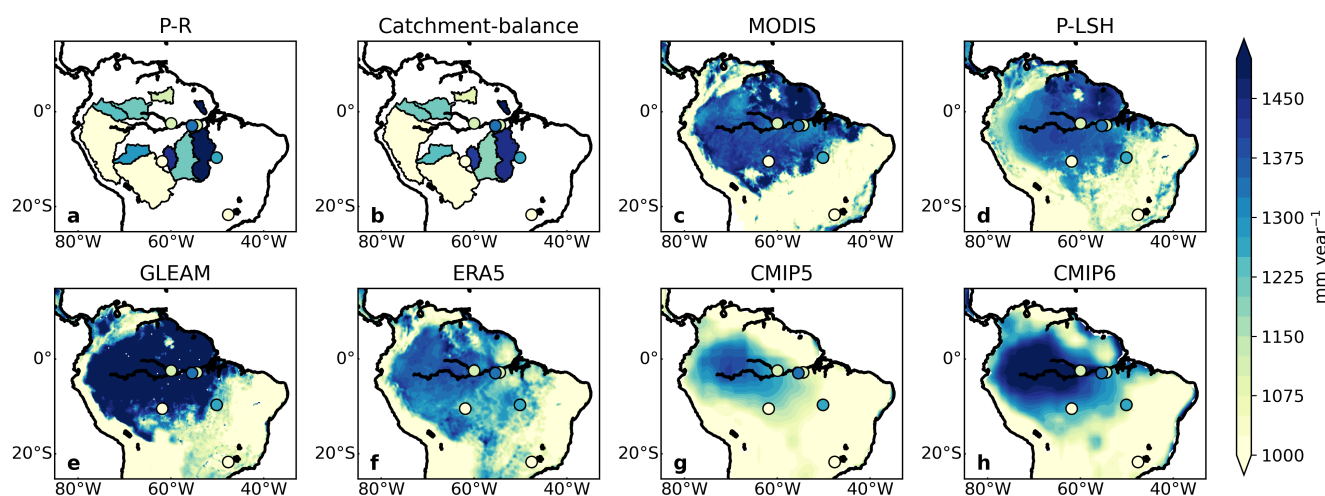
Figure 3 – Spatial variation in Amazon evapotranspiration from different approaches. Climatological mean annual ET from (a) differencing precipitation and runoff, (b) catchment-balance analysis accounting for change in groundwater storage, (c–e) satellite-based ET products, (f) ERA5 reanalysis, and (g, h) climate models. Coloured circles on each panel indicate ET
345   measured at six flux tower sites. Where there were multiple tower sites in close proximity, circles were plotted with an offset of 0.5° to improve data visualisation. Data for panels a–f and h are from 2003–2013, data for panel g are from 1994–2004 and flux-tower data are from the periods shown in Table S3. GLEAM data are presented with an alternative scale in Figure S5.

MODIS and P-LSH captured a northeast to southwest gradient in ET across the basin that was evident in the water-balance
350   approaches, showing highest ET over the Guiana shield in the north of the Amazon and decreasing southwest across the basin (Fig. 3c, d). Catchment-mean ET values from these two products were strongly correlated with ET from the catchment-balance approach across the eleven basins analysed in this study (r=0.84, p<0.01 and r=0.82, p<0.01 for MODIS and P-LSH, respectively), though spatial variability was weaker and interannual variability was also strongly underestimated (Fig. S6, Tables 2 and S7). Flux tower ET measurements, although spatially limited, showed a similar gradient in Amazon ET, with the
355   highest annual values over forest and seasonally-flooded sites in the east of the basin (coloured circles in Fig. 3). However, the gradient in tower data should be interpreted with some caution, since variation in energy-balance closure between sites will affect the absolute ET values (da Rocha et al., 2009b, Fisher et al., 2009). ET from GLEAM, which exceeded 1400 mm year⁻

[1] over much of the Amazon, showed a north-south ET gradient (Fig. 3e, see Fig S5 for alternative scale), and a positive, though not statistically significant, correlation with catchment-balance estimates (r=0.51, p=0.11, Fig. S6, Table S7). Previous studies

360 based on flux-tower measurements (Fisher et al., 2009), water-budget analysis (Zeng et al., 2012, Maeda et al., 2017, Sun et al., 2019), and a combination of satellites and flux towers (Paca et al., 2019) showed similar north/northeast to south/southwest gradients in ET across the Amazon, in line with the catchment-balance results presented in Figure 3.

ET from ERA5, CMIP5 and CMIP6 bore no relation to catchment-balance ET, simulating the highest ET values in the

365 northwest of the basin and decreasing to the east (Fig. 3e–g). The CMIP models do not incorporate any observations, and therefore might not be expected to perform as well the other products analysed in this study. However, an analysis of Amazon precipitation in 11 CMIP5 models found that most were able to capture spatial patterns relatively well, including shifting distributions through the course of the seasonal cycle (Yin et al., 2013). The poor representation of spatial variation in Amazon ET in reanalysis and coupled models shown in Figure 3 demonstrates a need for improvement of this key hydrological variable

370 in these products.

To understand the drivers of spatial variation in Amazon ET, we compared catchment-scale estimates against catchment-means of precipitation, surface radiation and LAI (Fig. 4). Since there were only eleven data points in the analysis (representing the Amazon and ten sub-catchments), statistical power was relatively low. However, we found spatial variation in catchment-

375 balance ET could largely be explained by variation in LAI (r=0.57, p=0.06, Fig. 4o), with some indication of an influence from radiation (r=0.38, p=0.25, Fig. 4h), but not precipitation (r=0.14, p=0.68, Fig. 4a). This result indicates that water availability is not a limiting factor controlling the spatial distribution of ET over the Amazon. All of the ET products and models analysed captured positive relationships between catchment-scale ET and LAI (Fig. 4o–u), though the strength of correlations was generally higher than seen for catchment-balance ET. Larger differences were observed in precipitation-ET and radiation-ET

380 relationships across catchments. ET from GLEAM, ERA5 and the CMIP ensembles all showed strong, positive, statistically significant relationships with precipitation (Fig. 4d–g), while spatial variation in ERA5 and CMIP5 ET was inversely related to radiation (Fig. 4l, m), i.e. the opposite to results from catchment balance. These results confirm that the reanalysis and climate models analysed here struggle to capture spatial patterns in Amazon ET due to misrepresentation of the controlling drivers, specifically the relative importance of precipitation and net radiation.
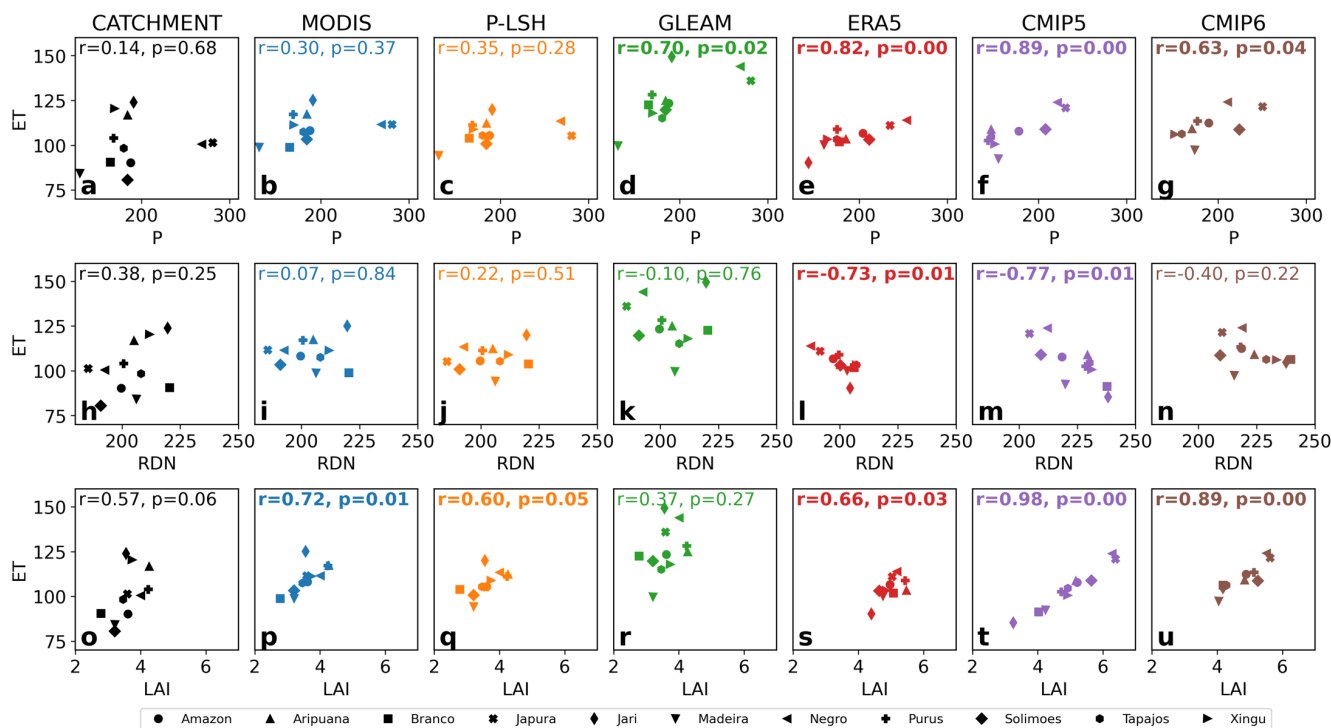
385

Figure 4 – Controls on spatial variation in Amazon evapotranspiration. Annual mean ET (in mm month[-1]) for the Amazon and ten sub-catchments (Fig. 1) from catchment-balance, satellites (MODIS, P-LSH, GLEAM), ERA5 reanalysis, and climate models (CMIP5 and CMIP6), plotted against (a–g) precipitation (P, mm month[-1]); (h–n) surface shortwave radiation (RDN, W m^{-2}); and (o–u) leaf area index (LAI, m[2] m^{-2}). Satellite ET data are plotted against P from CHIRPS, RDN from CLARA-A1

390 and LAI from MODIS; ERA5 and climate model ET are plotted against ERA5 and model P, RDN and LAI, respectively. Data are from 2003 to 2013, with the exception of CMIP5, where the data are from 1994–2004. Note that the axes do not start at zero.

For further insights on the validity of Amazon ET products and the factors controlling ET, we evaluated ET responses to spatial

395 variation in precipitation, radiation and LAI at the grid-cell level (Fig. 5). Differences between ET products were most apparent in their responses to annual precipitation (Fig. 5a). Above 2000 mm yr^{-1} datasets followed three patterns of behaviour: GLEAM ET continued to increase to approximately 1600 mm yr^{-1}, ET from MODIS, P-LSH and ERA5 remained relatively stable at around 1300 mm yr^{-1}, and CMIP5 and CMIP6 showed slight reductions in ET with further increases in precipitation. The precipitation threshold of 2000 mm yr^{-1} has previously been suggested as the level above which tropical forests are able to

400 sustain photosynthesis during the dry season (Guan et al., 2015), and as the breakpoint between productivity in the Amazon being water (< 2000 mm yr^{-1}) or radiation (> 2000 mm yr^{-1}) limited (Ahlström et al., 2017). Indeed, below 2000 mm yr^{-1} ET increased with increasing precipitation for all satellite, reanalysis and model datasets (lines in Fig. 5a), indicating a water-

limitation on ET. The two catchments in the northwest Amazon where P exceeds 3000 mm yr^{-1}, Japura and Negro, were most closely aligned with the products that showed ET levelling off when precipitation exceeded 2000 mm yr^{-1} (i.e. MODIS, P-

405   LSH and ERA5), suggesting these products represent the ET response to rainfall in very wet areas relatively well. For MODIS and P-LSH, this finding provides additional support that spatial patterns in Amazon ET correspond well with spatial variation in its controlling variables. In contrast, although ERA5 generally captured the correct ET response to precipitation (Fig. 5a), there are spatial differences between satellite and ERA5 precipitation datasets in Amazon regions with rainfall above 2000 mm yr^{-1} (Fig. S7). This explains why relationships between ERA5 precipitation and ET differed at the catchment (Fig. 4e) and

410   the grid-cell (Fig. 5a) scales. In the GLEAM model, the 'stress factor' that is used to scale PET takes precipitation as an input variable to the soil module (Table 1), which in turn controls the amount of water available for ET (Martens et al., 2017). Our results indicate that the GLEAM model overestimates the dependence of ET on soil moisture in regions with high annual rainfall, highlighting a possible target for improvements to the GLEAM algorithm.
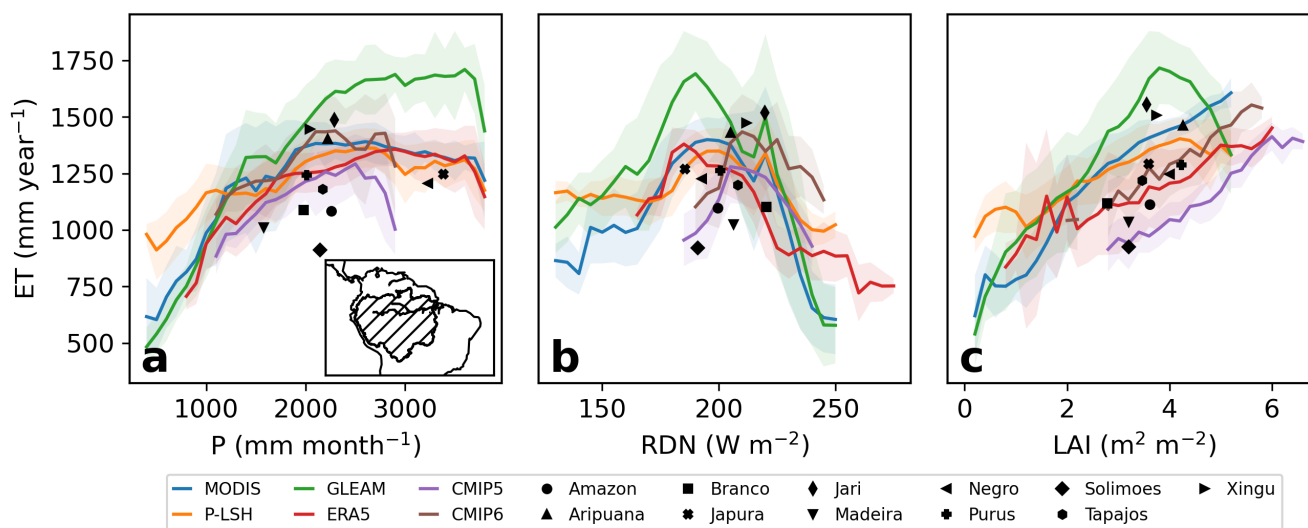
415

Figure 5 – ET response to spatial variation in controls. ET data from satellites (MODIS, P-LSH, GLEAM), ERA5 reanalysis, climate models (CMIP5 and CMIP6), and catchment-balance (black markers) are plotted against annual (a) precipitation (P); (b) surface shortwave radiation (RDN); and (c) leaf area index (LAI). Shading represents the standard deviation of the mean. Satellite ET data are plotted against P from CHIRPS, RDN from CLARA-A1 and LAI from MODIS;

420   ERA5 and climate model ET are plotted against ERA5 and model P, RDN and LAI, respectively. Data were extracted from the Amazon region indicated in the inset map in panel a. The locations of the catchments and tower sites are indicated in Figure 1. Data are from 2003 to 2013, with the exception of CMIP5, where the data are from 1994–2004. Note that the axes do not start at zero.

425 Differences between ET products in their relationships with other variables were more subtle. ET dependence on radiation was broadly similar among datasets, showing a peak at approximately 200 W m^{-2} (Fig. 5b). This is consistent with low and high levels of radiation tending to correspond with high and low levels of precipitation, respectively, and ET peaking at an optimum between the two. LAI-ET relationships were also fairly consistent, although GLEAM generally tended to overestimate ET relative to LAI, while CMIP5 tended to underpredict ET for a given LAI value (Fig. 5c), in comparison with ET from other

430 products and catchment-balance estimates.

Table 2 – Summary of comparative statistics. Datasets listed in the table were correlated with catchment-balance ET estimates (spatial, seasonal and interannual), and interannual standard deviations (σ) were calculated over the period 2003–2013 using data standardised by the climatological mean over that period (units of mm month^{-1} year^{-1}). Statistically significant

435 ($p<0.05$) relationships are shown in bold. Note that CMIP data were not correlated at the interannual scale because model years would not be expected to align with real-world years.

ET dataset	Spatial	Seasonal	Interannual variability, correlations with catchment balance and trends over 2003–2013 (mm month^{-1} year^{-1})								
	Climatological catchment means	Amazon	Annual			Wet (JFM)			Dry (JAS)		
			σ	r	Slope	σ	r	Slope	σ	r	Slope
Catchment-balance	-	-	2.90	-	-0.09	8.89	-	-0.74	8.92	-	0.15
MODIS	**0.84**	**0.63**	2.28	-0.24	**-0.58**	5.56	0.19	**-1.30**	5.01	-0.34	0.23
P-LSH	**0.82**	**0.67**	1.37	-0.11	**0.41**	1.83	0.00	-0.05	4.09	-0.09	**0.88**
GLEAM	0.51	-0.18	1.36	-0.42	0.09	1.82	-0.44	0.07	4.90	-0.36	0.41
ERA5	-0.28	**0.61**	0.65	0.13	0.05	1.91	0.01	-0.30	1.21	**-0.51**	-0.11
CMIP5	-0.06	-0.11	-	-	-	-	-	-	-	-	-
CMIP6	-0.14	0.05	0.48	-	0.02	0.37	-	0.05	1.48	-	0.07

3.2 Seasonal variation in Amazon ET

The mean seasonal cycle in Amazon ET was estimated from catchment-balance analysis, satellite, reanalysis and model ET

440 datasets for the whole Amazon, and for basins above and below the equator (Fig. 6). Amazon catchment-balance ET showed a strong seasonal cycle (standard deviation, σ = 22 mm month^{-1}), with annual minima during April–June and maxima in August–October (Fig. 6a). ET at the K34 tower site, located in the central Amazon, showed a similar seasonal pattern to that over the wider basin (Fig. S8), though intra-annual variation was weaker (σ = 14 mm month^{-1}). Furthermore, we observed strong, positive correlations between ET and radiation for the Amazon basin and K34 tower site (r=0.93, p<0.001 and r=0.68,

445 p<0.05, respectively, Figs. 7h, S9), and between ET and LAI for the basin (r=0.61, p<0.05, Fig. 7o), indicating controls on

seasonal ET are similar to controls on spatial variation in Amazon ET (Fig. 4h,o). These results agree with findings from da Rocha et al. (2009b), who made a detailed comparison of seasonal ET at seven flux tower sites in Brazil. They showed ET increased during the dry season at all four wet tropical forest sites (including K34), contrasting with three transition-forest and savanna sites where ET followed seasonal soil moisture availability. Studies based on catchment-balance analysis (Swann and

450 Koven, 2017), and satellite observations of vegetation photosynthetic properties (Guan et al., 2015) also showed that ET and forest productivity peak during the drier part of the year over the majority of the Amazon. Finally, our results are also consistent with those from Fisher et al. (2009), who identified radiation and NDVI as the primary and secondary controls on ET across the tropics based on analysis of flux tower measurements.

455
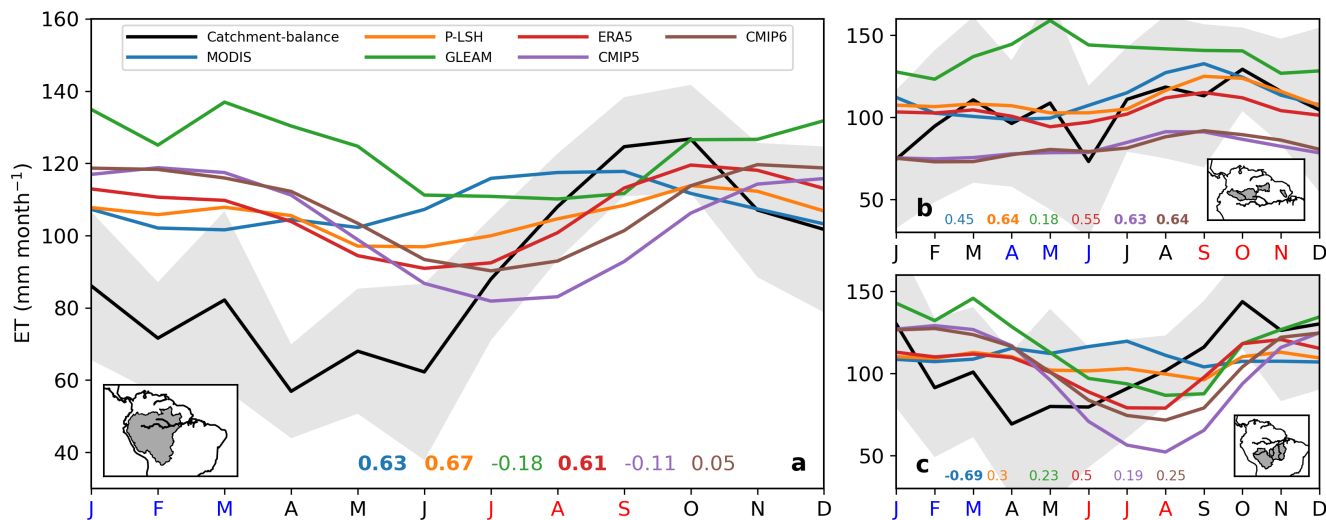
Figure 6 – Climatological seasonal cycles in evapotranspiration over the Amazon. Mean seasonal cycle in ET from catchment balance, satellites (MODIS, P-LSH, GLEAM), ERA5 reanalysis and climate models (CMIP5 and CMIP6) over the Amazon region drained by Óbidos (a), northern basins (b) and southern basins (c). The regions used in each analysis are

460 indicated in the inset maps. Shading represents absolute uncertainty in catchment-balance ET (see Methods). Correlations with catchment-balance ET are shown on each panel, with bold numbers indicating statistical significance (p<0.05). Data are from 2003 to 2013, with the exception of CMIP5, where the data are from 1994–2004. On the x-axis of each panel, the three wettest months are indicated in blue and three driest months are indicated in red. Note that the axes do not start at zero.

465 Monthly ET cycles from MODIS, P-LSH and ERA5 correlated with Amazon catchment ET (r=0.61–0.67, p<0.05, Table 2, Fig. 6a), and captured positive relationships with surface radiation (r=0.66–0.78, p<0.05, Fig. 7). However, despite representing the direction of seasonal fluctuations relatively well, these datasets underestimated the seasonal variability by 39– 77 %, relative to catchment-balance ET (Fig. 6a). Biases from catchment-balance ET were generally strongly positive from

January to June and weakly negative in September and October. At K34, MODIS and ERA5 overestimated the seasonal ET
470   range by 61 and 28 %, respectively, while P-LSH underestimated the range by 26% (Fig. S8). With such poor representation
of the magnitude of seasonal variability, and inconsistencies in the direction of amplitude biases, ET from these satellite and
reanalysis datasets may be of limited use for assessing long-term changes in the seasonality of the Amazon hydrological cycle
(Gloor et al., 2013), or for evaluating seasonal ET representation in coupled climate models.

475   ET from GLEAM, CMIP5 and CMIP6 neither correlated with seasonal catchment-balance Amazon ET, nor captured the
correct seasonal amplitude (Figs. 6a, 7, Table 2). Instead, ET from these datasets followed the same seasonal cycle as
precipitation, peaking during the wettest part of the year. A previous study comparing Amazon ET estimates derived using
different methods also observed that climate model and reanalysis ET tended to follow the precipitation seasonal cycle, with
annual ET minima in the dry season (Werth and Avissar, 2004). The authors suggested this was due to a strong vegetation
480   control on modelled ET due to down-regulation of stomatal conductance in the dry season, concluding such a control to be as
credible as a radiation control on Amazon ET. However, a subsequent study queried this assertion, citing evidence from flux
towers as proof that vegetation controls on Amazon ET were secondary to environmental controls (Costa et al., 2004). The
results presented in Figure 6a indicate a disconnect between our mechanistic understanding of the controls on seasonal Amazon
ET based on catchment-balance analysis, and the algorithms used to predict ET in GLEAM and the CMIP models.

485

Northern and southern Amazon sub-basins were analysed separately, due to differences in the timing of the seasonal
precipitation cycle above and below the equator (Fig. 6b,c). The seasonal cycle in catchment-balance ET was weaker in the
north than the south (σ=16 vs. 26 mm month^{-1}, respectively), following the pattern of precipitation seasonality, which is also
much larger (σ=69 vs. 115 mm month^{-1} in northern and southern basins, respectively). In general, satellite, reanalysis and
490   climate model ET related fairly well to seasonal catchment-balance ET in the northern Amazon (Fig. 6b), but showed much
weaker relationships in the southern Amazon (Fig. 6c). The CMIP5 and CMIP6 models, which were unable to capture seasonal
ET variation over the whole Amazon or southern Amazon (Fig. 6a,c), replicated month-to-month variations in ET over the
northern Amazon well, although both model groups underestimated seasonal variability (Fig. 6b). MODIS, which captured
seasonal ET over the whole Amazon (Fig. 6a), performed especially poorly in the south, showing a negative relationship with
495   catchment-balance ET (r=–0.57 p=0.06, Fig. 6c). These results highlight that the ability of ET products to capture seasonal ET
varies regionally, and a product that performs well over one region may not be reliable elsewhere.
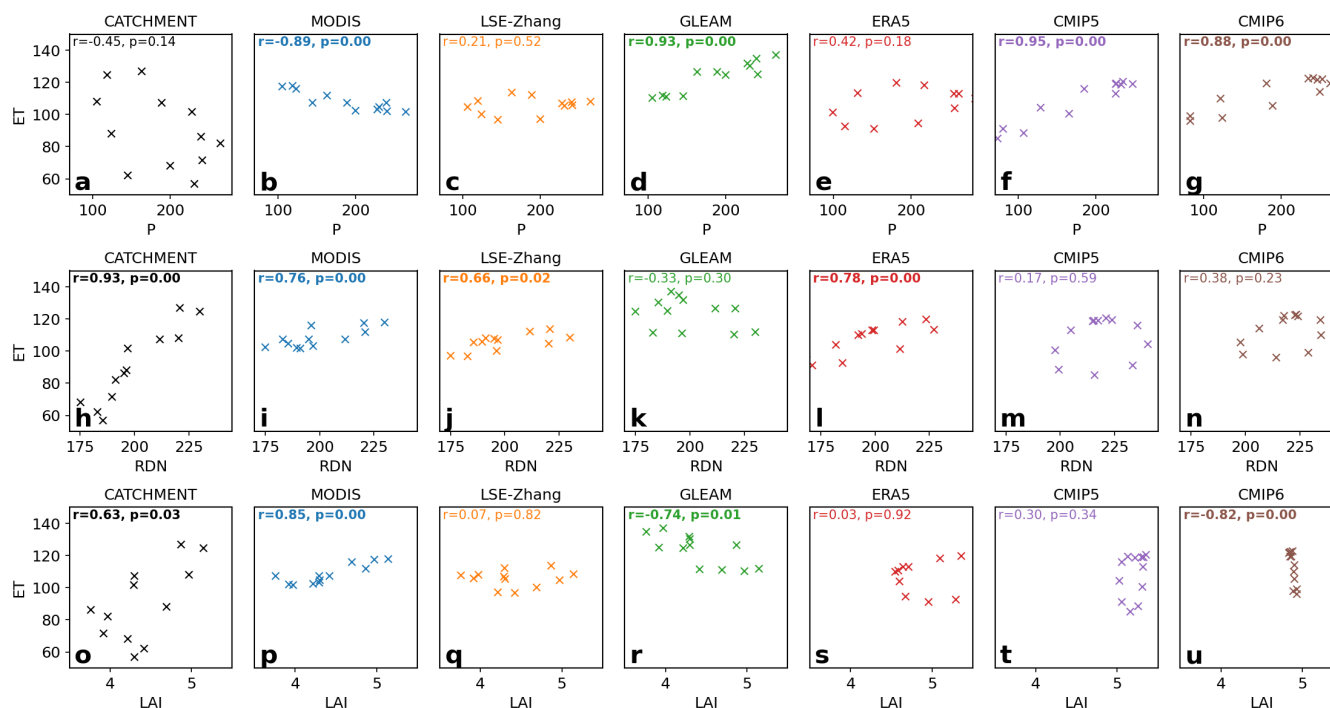
Figure 7 – Controls on seasonal variation in Amazon evapotranspiration. Monthly ET (in units of mm month[-1]) for the Amazon region drained by Óbidos (see Fig. 1) from catchment-balance, satellites (MODIS, P-LSH, GLEAM), ERA5 reanalysis, and climate models (CMIP5 and CMIP6) plotted against (a–g) precipitation (P, mm month[-1]); (h–n) surface shortwave radiation (RDN, W m^{-2}); and (o–u) leaf area index (LAI, m[2] m^{-2}). Satellite ET data are plotted against P from CHIRPS, RDN from CLARA-A1 and LAI from MODIS; ERA5 and climate model ET are plotted against ERA5 and model P, RDN and LAI, respectively. Data are from 2003 to 2013, with the exception of CMIP5, where the data are from 1994–2004. Note that the axes do not start at zero.

3.3 Interannual variation and trend analysis

Interannual time series of Amazon ET from 2001 to 2019 for the whole year, the three wettest months (January–March, JFM, see Fig. S9) and the three driest months (July–September, JAS), are shown in Figure 8. From 2003 to 2013, interannual variability (σ) in catchment-balance ET was 2.9 mm month[-1], or 3.2 % of the climatological mean. This value is comparable to the interannual variation in precipitation over the same period (σ=3.6 %), half the variation in runoff (σ=7.0 %) and represents around a tenth of the seasonal variation in Amazon ET (Fig. 6). With only a relatively short time series, controls on interannual variability were hard to detect, though radiation appeared to play a role (Fig. S10). Interannual variation was underestimated in ET from satellites, reanalysis and climate models by up to a factor of six relative to catchment-balance (Fig. 8a, Table 2). In JFM and JAS, ET variation was higher than at the annual scale (catchment-balance σ = 8.89 and 8.91 mm month[-1], respectively) and similarly underestimated by other datasets (Fig. 8b,c, Table 2). Relationships between interannual

515   catchment-balance ET and ET from satellites or reanalysis were generally poor (Table 2), and an especially high JFM

catchment-balance ET recorded in 2016, coinciding with a severe El Niño event (Koren et al., 2018), was not captured by

other ET products (Fig. 8b). ERA5 and CMIP6 showed the least interannual variation, indicating poor model representation

of the factors influencing inter-year changes in ET.

520   **Table 3 – Interannual trends in Amazon ET.** Linear trends in annual, January–March (JFM) and July–August (JAS) ET

were calculated over the time period common to all datasets (2003–2013) and for all years with available data in the past two

decades (units of mm month-1 year-1). Statistically significant (p<0.05) trends are shown in bold.

ET dataset	Time period	Annual		JFM		JAS	
		Slope	**p-value**	**Slope**	**p-value**	**Slope**	**p-value**
Catchment-balance	2003–2013	-0.09	0.77	-0.74	0.43	0.15	0.88
	2003–2019	-0.01	0.97	0.27	0.66	-0.51	0.28
MODIS	2003–2013	**-0.58**	**0.00**	**-1.30**	**0.01**	0.23	0.68
	2001–2019	-0.21	0.07	**-0.52**	**0.04**	0.21	0.38
P-LSH	2003–2013	**0.41**	**0.00**	-0.05	0.80	**0.88**	**0.02**
	2001–2013	**0.32**	**0.00**	-0.01	0.94	**0.63**	**0.03**
GLEAM	2003–2013	0.09	0.56	0.07	0.74	0.41	0.43
	2003–2017	-0.32	0.09	**-0.50**	**0.02**	0.12	0.73
ERA5	2003–2013	-0.05	0.47	-0.30	0.13	-0.11	0.40
	2001–2019	0.01	0.86	**-0.27**	**0.03**	0.03	0.69
CMIP6	2003–2013	0.02	0.77	0.05	0.15	0.07	0.66
	2001–2014	0.00	0.96	0.03	0.42	-0.02	0.88
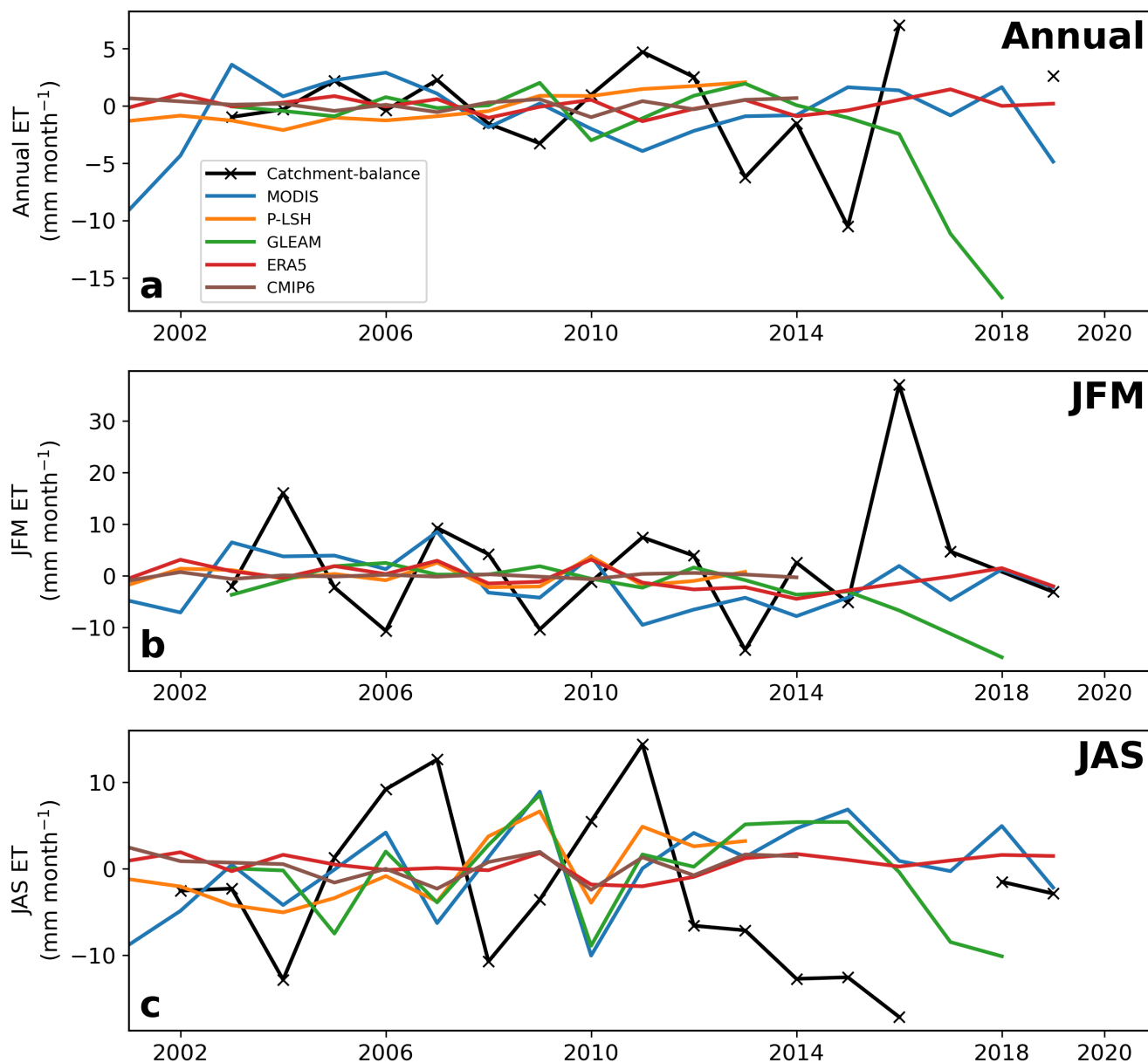
Figure 8 – Interannual variation in evapotranspiration from 2001 to 2019. Time series in ET over the Amazon from catchment balance (black, region drained by Óbidos, Fig. 1), satellites (MODIS, P-LSH, GLEAM), ERA5 reanalysis and CMIP6 models, for (a) the whole year, (b) January–March (JFM) and (c) July–September (JAS), normalised by the 2003–2013 climatological mean. Interannual trends are listed in Table 3.

Finally, we assessed interannual trends in Amazon ET over the common time period of 2003–2013, and using all years of available data for each dataset (Table 3). No statistically significant temporal trends were observed for annual, JFM or JAS catchment-balance ET over the respective periods analysed. Removal of the anomalous El Niño year had no impact on the results. Previous studies based on the P-LSH satellite product (Zhang et al., 2015a), and other satellite ET products and

535   machine-learning approaches (Zhang et al., 2016b, Pan et al., 2020) have reported multi-decadal increases in ET, globally and over the Amazon, from the early 1980s to the early 2010s, due to long-term warming driving increased evaporative demand. Meanwhile, climate models predict that Amazon ET will decrease over the next century due to reductions in plant stomatal conductance driven by rising atmospheric CO_2 (i.e. the CO_2 fertilisation effect), leading to declines in Amazon rainfall (Skinner et al., 2017, Kooperman et al., 2018, Langenbrunner et al., 2019). Swann and Koven (2017) had observed a statistically-

540   significant reduction in monthly catchment-balance Amazon ET from 2002–2016 (-0.12 mm month^{-1} year^{-1}), which they hypothesised may have been driven by a reduction in Amazon precipitation, deforestation, or CO_2 fertilisation. Our catchment-balance ET data, analysed over a similar period but at the annual timescale, gave a similar value (i.e. -0.09 mm month^{-1} year^{-1}, 2003–2013, Table 3), though the result was not statistically significant due to the short length of the time series. Extension of the record to 2019 reduced the magnitude of the trend to approximately zero (Table 3). The absence of a discernible trend

545   in catchment-balance ET in this study suggests that previously reported positive trends in Amazon ET may have levelled off, but that there has not yet been a systematic shift towards long-term reductions in ET driven by precipitation, deforestation or the CO_2 fertilisation effect, over the portion of the Amazon drained by Óbidos (Fig. 1), with the caveat that ET changes over the eastern portion of the basin would not be detected in our approach.

550   Among other datasets, there was little agreement in the direction of ET trends, with both positive and negative trends detected at the annual timescale (P-LSH and MODIS, respectively), and only one product showing a statistically significant upward trend in JAS ET (P-LSH, Table 3). There was more agreement in JFM, with MODIS, GLEAM and ERA5 all showing modest declines in ET (-0.27 to -1.3 mm month^{-1} year^{-1}, variable time periods, Table 3). Trends in satellite-derived climate datasets can occur from gradual changes in the satellite orbit over time (drift), which could explain some of the observed trend

555   disparities, although such artefacts should have been corrected for during data processing (Gutman, 1999, Pinzón et al., 2005). Overall, the inconsistencies between satellite, reanalysis and climate model ET records at the interannual timescale, and poor correspondence with catchment-balance ET, highlight that current products are inadequate for evaluating long-term changes in Amazon ET. Given that changes in ET have major implications for regional climate and the sustainability of the Amazon forest biome, there is a clear need for further long-term ground measurements of ET in the region, including direct measures

560   such sap-flow.

4 Summary and conclusions

This study aimed to collate estimates of Amazon ET from water-budget analysis, remote sensing, reanalysis, flux-tower measurements and coupled climate models to identify key characteristics of the regional hydrological cycle, compare and evaluate datasets, and identify remaining gaps in our understanding of this important variable. Our quantification of Amazon

565 ET from terms in the water-budget equation revealed a clear spatial gradient in annual ET from east/northeast to west/southwest across the Amazon, consistent with measurements from flux towers. We observed a strong seasonal cycle in Amazon-wide ET peaking in August–October, and no evidence of a long-term trend in annual, January–March or July–September ET from 2001 to 2019. Spatial, seasonal and (to a lesser degree) interannual variation in ET was shown to be governed by surface radiation and LAI, highlighting the main factors controlling surface water fluxes in the Amazon region.

570

The catchment-balance approach, although providing a relatively direct measure of ET, still has a degree of associated uncertainty (Table S2), and assumes complete closure of the water budget. In particular, subsurface runoff to other catchments and anthropogenic hydrological management could potentially impact the R term in equation 1 (Miralles et al., 2016). Incorporating groundwater measurements, as applied here, should account for sub-surface runoff. However, human

575 encroachment on the Amazon hydrological regime has risen in recent decades with the expansion of hydropower impacting river flow patterns and flood pulse frequency (Fearnside, 2014, Timpe and Kaplan, 2017). ET estimates for the Aripuanã and whole-Amazon river catchments may have been affected by dam development, though our focus on temporal means made it less likely that our findings were affected by human-induced perturbations to monthly river flows. Furthermore, the generally good agreement between our results and those from previous studies using different data inputs (e.g. Swann and Koven, 2017)

580 provides confidence that our approach was robust.

Performance of satellite, reanalysis and climate model ET was highly variable, though all products overestimated ET at the annual scale (15–37 %), while substantially underestimating temporal variability relative to catchment-balance. In general, satellite ET estimates based on the Penman-Monteith equation (MODIS and P-LSH) showed the best correspondence with

585 catchment-balance ET, mostly capturing spatial and seasonal patterns of variation. The satellite-based GLEAM ET product showed strong positive relationships with rainfall even over very wet parts of the Amazon, suggesting an over-dependence on soil moisture in the GLEAM land-surface model. ERA5 reanalysis ET performed well at the seasonal scale, and mostly captured the correct relationships with factors controlling ET. However, misrepresentation of other reanalysis variables, including the spatial distribution of precipitation over the Amazon, detrimentally affected ERA5 ET. The CMIP5 and CMIP6

590 models struggled to capture major features of Amazon ET, including spatial and seasonal variability. CMIP6, which represents the latest generation of coupled climate models, showed little evidence of improvement in the representation of Amazon ET compared to CMIP5. It has been suggested that errors in model rooting (Pan et al., 2020) and soil depth (Baker et al., in review

at NCC) could play a role in the mischaracterisation of simulated Amazon ET, highlighting possible areas for future model development.

595

Finally, correspondence between ET products at the interannual timescale was particularly poor, suggesting they are currently inadequate for monitoring long-term trends in Amazon ET. The future of Amazon ET has implications for regional climate and, therefore, the fate of the Amazon rainforest, with its rich biodiversity and valuable stores of terrestrial carbon (Malhi et al., 2008, Zhang et al., 2015b). However, uncertainty remains over the direction of future ET trends, with climate warming

600 and increasing LAI promoting ET increases (Kergoat et al., 2002, Zhang et al., 2015a), and deforestation and CO_2-induced reductions in sap flow forcing declines in ET (Zemp et al., 2017b, Skinner et al., 2017, Baker and Spracklen, 2019). Discrepancies in the direction of trends from different ET products in this study make it difficult to assess which of these opposing mechanisms are in operation. Furthermore, deficiencies in the representation of ET in CMIP5 and CMIP6 models highlighted here raise questions over the reliability of Amazon ET projections over the next century, with implications for

605 other regions. Until models are better able to capture historical patterns of ET and its controlling variables, attempts to understand future changes in the Amazon hydrological cycle will be severely hampered.

5 Data and code availability

The observational, reanalysis, model and flux-tower datasets analysed in the study are available in the following repositories:

- CHIRPS precipitation: https://www.chc.ucsb.edu/data/chirps
610
- Amazon river-gauge station data: http://www2.ana.gov.br/Paginas/EN/default.aspx
- GRACE terrestrial water storage: https://grace.jpl.nasa.gov/data/get-data/jpl_global_mascons/
- MODIS ET: https://lpdaac.usgs.gov/products/mod16a2v006/
- P-LSH ET: https://www.ntsg.umt.edu/project/global-et.php
- GLEAM ET: https://www.gleam.eu
615
- ERA5 reanalysis: https://climate.copernicus.eu/climate-reanalysis
- CMIP5 and CMIP6 historical simulations: https://esgf-data.dkrz.de/projects/esgf-dkrz/
- CLARA-A1 radiation: https://wui.cmsaf.eu/safira/action/viewDoiDetails?acronym=CLARA_AVHRR_V001
- MODIS leaf area index: https://lpdaac.usgs.gov/products/mod15a2hv006/
- LBA-ECO flux tower data: https://daac.ornl.gov/LBA/guides/CD32_Brazil_Flux_Network.html
620

We have uploaded a dataset containing Amazon catchment-scale estimates of ET, P, RDN and LAI for 2003–2013 from the data sources described in this study to an online repository (10.5281/zenodo.4271331). All of the scripts used to process the

raw data files are available here: https://github.com/jcabaker/amazon_et. Python scripts used for data analysis in this study are available from the authors upon request.

6 Author contributions

JB, LGC, MG, JM, WB and DS devised the study, planned the analysis and discussed the results. HR, AN and AA provided ET data, and expertise on Amazon flux-tower measurements. JB performed the analysis and wrote the paper. All authors provided feedback on the manuscript.

7 Competing interests

The authors declare that they have no conflict of interest.

8 Acknowledgements

The research has been supported by funding from the European Research Council (ERC) under the European Union's Horizon 2020 research and innovation programme (DECAF project, Grant agreement no. 771492), a Natural Environment Research Council standard grant (NE/K01353X/1), and the Newton Fund, through the Met Office Climate Science for Service Partnership Brazil (CSSP Brazil). The authors also thank contributors to the LBA-ECO Brazil Flux Tower Network for their valuable efforts measuring evapotranspiration in the Amazon and for sharing their data with the scientific community.

9 References

Studies in prep or in review

Baker, J.C.A., Garcia-Carreras, L., Buermann, W., Castilho de Souza, D., Marsham, J.H., Kubota, P., Gloor, M., Coelho, C.A.S. & Spracklen, D.V. *In review at Nature Climate Change*. Robust Amazon precipitation projections in models that capture land-atmosphere feedbacks.
Baker, J.C.A., Castilho de Souza, D., Kubota, P., Buermann, W., Coelho, C.A.S., Andrews, M.B., Gloor, M., Garcia-Carreras, L., Figueroa, S.N. & Spracklen, D.V. *In review at Journal of Hydrometeorology*. Land-atmosphere moisture coupling over South America in simulations from the UK and Brazil climate models.

Published studies

Ahlström, A., Canadell, J. G., Schurgers, G., Wu, M., Berry, J. A., Guan, K. & Jackson, R. B. 2017. Hydrologic resilience and Amazon productivity. *Nature Communications,* 8**,** 387.
Baker, J. C. A. & Spracklen, D. V. 2019. Climate Benefits of Intact Amazon Forests and the Biophysical Consequences of Disturbance. *Frontiers in Forests and Global Change,* 2.

Callède, J., Ronchail, J., Guyot, J.-L. & Oliveira, E. D. 2008. Déboisement amazonien: son influence sur le débit de l'Amazone à Óbidos (Brésil). *Revue des sciences de l'eau/Journal of Water Science,* 21**,** 59-72.

Christoffersen, B. O., Restrepo-Coupe, N., Arain, M. A., Baker, I. T., Cestaro, B. P., Ciais, P., Fisher, J. B., Galbraith, D., Guan, X. D., Gulden, L., Van Den Hurk, B., Ichii, K., Imbuzeiro, H., Jain, A., Levine, N., Miguez-Machor, G.,
655   Poulter, B., Roberti, D. R., Sakaguchi, K., Sahoo, A., Schaefer, K., Shi, M. J., Verbeeck, H., Yang, Z. L., Araujo, A. C., Kruijt, B., Manzi, A. O., Da Rocha, H. R., Von Randow, C., Muza, M. N., Borak, J., Costa, M. H., De Goncalves, L. G. G., Zeng, X. B. & Saleska, S. R. 2014. Mechanisms of water supply and vegetation demand govern the seasonality and magnitude of evapotranspiration in Amazonia and Cerrado. *Agricultural and Forest Meteorology,* 191**,** 33-50.

660 Costa, M. H., Souza-Filho, J. C. & Ribeiro, A. 2004. Comments on "The Regional Evapotranspiration of the Amazon". *Journal of Hydrometeorology,* 5**,** 1279-1280.

Costa, M. H., Biajoli, M. C., Sanches, L., Malhado, A. C. M., Hutyra, L. R., Da Rocha, H. R., Aguiar, R. G. & De Araújo, A. C. 2010. Atmospheric versus vegetation controls of Amazonian tropical rain forest evapotranspiration: Are the wet and seasonally dry rain forests any different? *Journal of Geophysical Research: Biogeosciences,* 115.

665 Da Rocha, H. R., Goulden, M. L., Miller, S. D., Menton, M. C., Pinto, L. D. V. O., De Freitas, H. C. & E Silva Figueira, A. M. 2004. Seasonality of water and heat fluxes over a tropical forest in eastern Amazonia. *Ecological Applications,* 14**,** 22-32.

Da Rocha, H. R., Manzi, A. O. & Shuttleworth, J. 2009a. Evapotranspiration. *Amazonia and Global Change.*

Da Rocha, H. R., Manzi, A. O., Cabral, O. M., Miller, S. D., Goulden, M. L., Saleska, S. R., R.-Coupe, N., Wofsy, S. C.,
670   Borma, L. S., Artaxo, P., Vourlitis, G., Nogueira, J. S., Cardoso, F. L., Nobre, A. D., Kruijt, B., Freitas, H. C., Von Randow, C., Aguiar, R. G. & Maia, J. F. 2009b. Patterns of water and heat flux across a biome gradient from tropical forest to savanna in Brazil. *Journal of Geophysical Research: Biogeosciences,* 114.

Da Silva, H. J. F., Gonçalves, W. A. & Bezerra, B. G. 2019. Comparative analyzes and use of evapotranspiration obtained through remote sensing to identify deforested areas in the Amazon. *International Journal of Applied Earth*
675   *Observation and Geoinformation,* 78**,** 163-174.

De Oliveira, G., Brunsell, N. A., Moraes, E. C., Shimabukuro, Y. E., Bertani, G., Dos Santos, T. V. & Aragao, L. 2017. Evaluation of MODIS-based estimates of water-use efficiency in Amazonia. *International Journal of Remote Sensing,* 38**,** 5291-5309.

Dingman, S. L. 2015. *Physical hydrology*, Waveland press.

680 Eltahir, E. A. & Bras, R. L. 1994. Precipitation recycling in the Amazon basin. *Quarterly Journal of the Royal Meteorological Society,* 120**,** 861-880.

Eltahir, E. A. 1996. Role of vegetation in sustaining large-scale atmospheric circulations in the tropics. *Journal of Geophysical Research,* 101**,** 4255-4268.

Eyring, V., Bony, S., Meehl, G. A., Senior, C. A., Stevens, B., Stouffer, R. J. & Taylor, K. E. 2016. Overview of the
685   Coupled Model Intercomparison Project Phase 6 (CMIP6) experimental design and organization. *Geoscientific Model Development.*

Fearnside, P. M. 2014. Viewpoint-Brazil's Madeira River Dams: A Setback for Environmental Policy in Amazonian Development. *Water Alternatives,* 7.

Fisher, J. B., Malhi, Y., Bonal, D., Da Rocha, H. R., De Araújo, A. C., Gamo, M., Goulden, M. L., Hirano, T., Huete, A. R.,
690   Kondo, H., Kumagai, T. O., Loescher, H. W., Miller, S., Nobre, A. D., Nouvellon, Y., Oberbauer, S. F., Panuthai, S., Roupsard, O., Saleska, S., Tanaka, K., Tanaka, N., Tu, K. P. & Von Randow, C. 2009. The land–atmosphere water flux in the tropics. *Global Change Biology,* 15**,** 2694-2714.

Foken, T. 2008. The Energy Balance Closure Problem: An Overview. *Ecological Applications,* 18**,** 1351-1367.

Funk, C., Peterson, P., Landsfeld, M., Pedreros, D., Verdin, J., Shukla, S., Husak, G., Rowland, J., Harrison, L., Hoell, A. &
695   Michaelsen, J. 2015. The climate hazards infrared precipitation with stations—a new environmental record for monitoring extremes. *Scientific Data,* 2**,** 150066.

Gat, J. R. & Matsui, E. 1991. Atmospheric water balance in the Amazon basin: An isotopic evapotranspiration model. *Journal of Geophysical Research: Atmospheres,* 96**,** 13179-13188.

Gloor, M., Brienen, R. J. W., Galbraith, D., Feldpausch, T. R., Schöngart, J., Guyot, J. L., Espinoza, J. C., Lloyd, J. &
700   Phillips, O. L. 2013. Intensification of the Amazon hydrological cycle over the last two decades. *Geophysical Research Letters,* 40**,** 1729-1733.

Good, S. P., Noone, D. & Bowen, G. 2015. Hydrologic connectivity constrains partitioning of global terrestrial water fluxes. *Science,* 349**,** 175-177.

Guan, K., Pan, M., Li, H., Wolf, A., Wu, J., Medvigy, D., Caylor, K. K., Sheffield, J., Wood, E. F., Malhi, Y., Liang, M.,
705   Kimball, J., Saleska, S., Berry, J., Joiner, J. & Lyapustin, A. 2015. Photosynthetic seasonality of global tropical forests constrained by hydroclimate. *Nature Geoscience,* 8**,** 284-289.

Gutman, G. G. 1999. On the monitoring of land surface temperatures with the NOAA/AVHRR: Removing the effect of satellite orbit drift. *International Journal of Remote Sensing,* 20**,** 3407-3413.

Hasler, N. & Avissar, R. 2007. What Controls Evapotranspiration in the Amazon Basin? *Journal of Hydrometeorology,* 8**,**
710   380-395.

Hersbach, H., Rosnay, P. D., Bell, B., Schepers, D., Simmons, A., Soci, C., Abdalla, S., Alonso-Balmaseda, M., Gianpaol, B., Bechtold, P., Berrisford, P., Bidlot, J.-R., E., D. B., Bonavita, M., P., B., Buizza, R., Dahlgren, P., Dee, D., Dragani, R., Diamantakis, M., Flemming, J., Forbes, R., Geer, A. J., Haiden, T., Hólm, E., Haimberger, L., Hogan, R., Horányi, A., M., J., Laloyaux, P., Lopez, P., Munoz-Sabater, J., Peubey, C., Radu, R., Richardson, D., Thépaut,
715   J.-N., Vitart, F., Yang, X., Zsótér, E. & Zuo, H. 2018. Operational global reanalysis: progress, future directions and synergies with NWP.

Hidroweb 2018. HidroWeb, Brazilian Water Resources Database. Water Resources National Agency, Brazil: Agência Nacional de Águas.

Huffman, G. J. 1997. Estimates of root-mean-square random error for finite samples of estimated precipitation. *Journal of*
720   *Applied Meteorology,* 36**,** 1191-1201.

Jasechko, S., Sharp, Z. D., Gibson, J., Birks, S. J., Yi, Y. & Fawcett, P. J. 2013. Terrestrial water fluxes dominated by transpiration. *Nature,* 496**,** 347-350.

Jasechko, S. 2018. Plants turn on the tap. *Nature Climate Change,* 8**,** 562-563.

Jung, M., Reichstein, M., Ciais, P., Seneviratne, S. I., Sheffield, J., Goulden, M. L., Bonan, G., Cescatti, A., Chen, J., De Jeu,
725   R., Dolman, A. J., Eugster, W., Gerten, D., Gianelle, D., Gobron, N., Heinke, J., Kimball, J., Law, B. E., Montagnani, L., Mu, Q., Mueller, B., Oleson, K., Papale, D., Richardson, A. D., Roupsard, O., Running, S., Tomelleri, E., Viovy, N., Weber, U., Williams, C., Wood, E., Zaehle, S. & Zhang, K. 2010. Recent decline in the global land evapotranspiration trend due to limited moisture supply. *Nature,* 467**,** 951-954.

Karlsson, K. G., Riihelä, A., Müller, R., Meirink, J. F., Sedlar, J., Stengel, M., Lockhoff, M., Trentmann, J., Kaspar, F.,
730   Hollmann, R. & Wolters, E. 2013. CLARA-A1: a cloud, albedo, and radiation dataset from 28 yr of global AVHRR data. *Atmos. Chem. Phys.,* 13**,** 5351-5367.

Keller, M., Bustamante, M., Gash, J. & Dias, P. S. 2009. *Amazonia and global change,* American Geophysical Union.

Kergoat, L., Lafont, S., Douville, H., Berthelot, B., Dedieu, G., Planton, S. & Royer, J.-F. 2002. Impact of doubled CO2 on global-scale leaf area index and evapotranspiration: Conflicting stomatal conductance and LAI responses. *Journal*
735   *of Geophysical Research: Atmospheres,* 107**,** ACL 30-1-ACL 30-16.

Khand, K., Numata, I., Kjaersgaard, J. & Vourlitis, G. L. 2017. Dry season evapotranspiration dynamics over human-impacted landscapes in the southern Amazon using the Landsat-based METRIC model. *Remote Sensing,* 9**,** 706.

Kooperman, G. J., Chen, Y., Hoffman, F. M., Koven, C. D., Lindsay, K., Pritchard, M. S., Swann, A. L. S. & Randerson, J. T. 2018. Forest response to rising CO2 drives zonally asymmetric rainfall change over tropical land. *Nature Climate*
740   *Change,* 8**,** 434-440.

Koren, G., Schaik, E. V., Araújo, A. C., Boersma, K. F., Gärtner, A., Killaars, L., Kooreman, M. L., Kruijt, B., Laan-Luijkx, I. T. V. D., Randow, C. V., Smith, N. E. & Peters, W. 2018. Widespread reduction in sun-induced fluorescence from the Amazon during the 2015/2016 El Niño. *Philosophical Transactions of the Royal Society B: Biological Sciences,* 373**,** 20170408.

745 Kunert, N., Aparecido, L. M. T., Wolff, S., Higuchi, N., Santos, J. D., Araujo, A. C. D. & Trumbore, S. 2017. A revised hydrological model for the Central Amazon: The importance of emergent canopy trees in the forest water budget. *Agricultural and Forest Meteorology,* 239**,** 47-57.

Langenbrunner, B., Pritchard, M. S., Kooperman, G. J. & Randerson, J. T. 2019. Why Does Amazon Precipitation Decrease When Tropical Forests Respond to Increasing CO2? *Earth's Future,* 7**,** 450-468.

750   Long, D., Longuevergne, L. & Scanlon, B. R. 2014. Uncertainty in evapotranspiration from land surface modeling, remote sensing, and GRACE satellites. *Water Resources Research,* 50**,** 1131-1151.

Maeda, E. E., Ma, X. L., Wagner, F. H., Kim, H., Oki, T., Eamus, D. & Huete, A. 2017. Evapotranspiration seasonality across the Amazon Basin. *Earth System Dynamics,* 8**,** 439-454.

Malhi, Y., Roberts, J. T., Betts, R. A., Killeen, T. J., Li, W. & Nobre, C. A. 2008. Climate change, deforestation, and the fate

755   of the Amazon. *Science,* 319**,** 169-172.

Marengo, J. A. 2006. On the hydrological cycle of the Amazon Basin: A historical review and current state-of-the-art. *Revista Brasileira de Meteorologia,* 21**,** 1-19.

Martens, B., Miralles, D. G., Lievens, H., Van Der Schalie, R., De Jeu, R. A., Fernández-Prieto, D., Beck, H. E., Dorigo, W. A. & Verhoest, N. E. 2017. GLEAM v3: satellite-based land evaporation and root-zone soil moisture. *Geoscientific*

760   *Model Development,* 10**,** 1903.

Martinelli, L. A., Victoria, R. L., Silveira Lobo Sternberg, L., Ribeiro, A. & Zacharias Moreira, M. 1996. Using stable isotopes to determine sources of evaporated water to the atmosphere in the Amazon basin. *Journal of Hydrology,* 183**,** 191-204.

Michel, D., Jiménez, C., Miralles, D. G., Jung, M., Hirschi, M., Ershadi, A., Martens, B., Mccabe, M. F., Fisher, J. B., Mu,

765   Q., Seneviratne, S. I., Wood, E. F. & Fernández-Prieto, D. 2016. The WACMOS-ET project – Part 1: Tower-scale evaluation of four remote-sensing-based evapotranspiration algorithms. *Hydrol. Earth Syst. Sci.,* 20**,** 803-822.

Miralles, D. G., Holmes, T. R. H., De Jeu, R. a. M., Gash, J. H., Meesters, A. G. C. A. & Dolman, A. J. 2011. Global land-surface evaporation estimated from satellite-based observations. *Hydrol. Earth Syst. Sci.,* 15**,** 453-469.

Miralles, D. G., Jiménez, C., Jung, M., Michel, D., Ershadi, A., Mccabe, M. F., Hirschi, M., Martens, B., Dolman, A. J.,

770   Fisher, J. B., Mu, Q., Seneviratne, S. I., Wood, E. F. & Fernández-Prieto, D. 2016. The WACMOS-ET project – Part 2: Evaluation of global terrestrial evaporation data sets. *Hydrol. Earth Syst. Sci.,* 20**,** 823-842.

Monteith, J. 1965. Evaporation and environment. The state and movement of water in living organisms. *Symposium of the Society of Experimental Biology,* 19**,** 205-234.

Moreira, M., Sternberg, L., Martinelli, L., Victoria, R., Barbosa, E., Bonates, L. & Nepstad, D. 1997. Contribution of

775   transpiration to forest ambient vapour based on isotopic measurements. *Global Change Biology,* 3**,** 439-450.

Mu, Q., Heinsch, F. A., Zhao, M. & Running, S. W. 2007. Development of a global evapotranspiration algorithm based on MODIS and global meteorology data. *Remote Sensing of Environment,* 111**,** 519-536.

Mu, Q., Zhao, M. & Running, S. W. 2011. Improvements to a MODIS global terrestrial evapotranspiration algorithm. *Remote Sensing of Environment,* 115**,** 1781-1800.

780   Mu, Q., Zhao, M. & Running, S. W. 2013. MODIS global terrestrial evapotranspiration (ET) product (NASA MOD16a2/a3). *Algorithm Theoretical Basis Document, Collection,* 5.

Mueller, B. & Seneviratne, S. I. 2014. Systematic land climate and evapotranspiration biases in CMIP5 simulations. *Geophysical Research Letters,* 41**,** 128-134.

Myneni, R., Knyazikhin, Y. & Park, T. 2015. MOD15A2H MODIS/Terra Leaf Area Index/FPAR 8-Day L4 Global 500 m

785   SIN Grid V006. *NASA EOSDIS Land Processes DAAC. Available online: https://lpdaac. usgs. gov/dataset_discovery/modis/modis_products_table/mod15a2h_v006 (accessed on 1 June 2017).*

Nepstad, D. C., Stickler, C. M., Filho, B. S.-. & Merry, F. 2008. Interactions among Amazon land use, forests and climate: prospects for a near-term forest tipping point. *Philosophical Transactions of the Royal Society B: Biological Sciences,* 363**,** 1737-1746.

790   Paca, V. H. D. M., Espinoza-Dávalos, G. E., Hessels, T. M., Moreira, D. M., Comair, G. F. & Bastiaanssen, W. G. M. 2019. The spatial variability of actual evapotranspiration across the Amazon River Basin based on remote sensing products validated with flux towers. *Ecological Processes,* 8**,** 6.

Pan, S., Pan, N., Tian, H., Friedlingstein, P., Sitch, S., Shi, H., Arora, V. K., Haverd, V., Jain, A. K., Kato, E., Lienert, S., Lombardozzi, D., Nabel, J. E. M. S., Ottlé, C., Poulter, B., Zaehle, S. N. & Running, S. W. 2020. Evaluation of

795   global terrestrial evapotranspiration using state-of-the-art approaches in remote sensing, machine learning and land surface modeling. *Hydrology and Earth System Sciences,* 24**,** 1485-1509.

Paredes-Trejo, F. J., Barbosa, H. A. & Lakshmi Kumar, T. V. 2017. Validating CHIRPS-based satellite precipitation estimates in Northeast Brazil. *Journal of Arid Environments,* 139**,** 26-40.

Pinzón, J. E., Brown, M. E. & Tucker, C. J. 2005. EMD CORRECTION OF ORBITAL DRIFT ARTIFACTS IN SATELLITE DATA STREAM. *Hilbert-Huang Transform and Its Applications.*

Priestley, C. & Taylor, R. 1972. On the assessment of surface heat flux and evaporation using large-scale parameters. *Monthly weather review,* 100**,** 81-92.

Restrepo-Coupe, N., Da Rocha, H. R., Hutyra, L. R., Da Araujo, A. C., Borma, L. S., Christoffersen, B., Cabral, O. M. R., De Camargo, P. B., Cardoso, F. L., Da Costa, A. C. L., Fitzjarrald, D. R., Goulden, M. L., Kruijt, B., Maia, J. M. F., Malhi, Y., Manzi, A. O., Miller, S. D., Nobre, A. D., Von Randow, C., Sá, L. D. A., Sakai, R. K., Tota, J., Wofsy, S. C., Zanchi, F. B. & Saleska, S. R. 2013. What drives the seasonality of photosynthesis across the Amazon basin? A cross-site analysis of eddy flux tower measurements from the Brasil flux network. *Agricultural and Forest Meteorology,* 182–183**,** 128-144.

Rodell, M. & Famiglietti, J. S. 1999. Detectability of variations in continental water storage from satellite observations of the time dependent gravity field. *Water Resources Research,* 35**,** 2705-2723.

Rodell, M., Mcwilliams, E. B., Famiglietti, J. S., Beaudoing, H. K. & Nigro, J. 2011. Estimating evapotranspiration using an observation based terrestrial water budget. *Hydrological Processes,* 25**,** 4082-4092.

Ruhoff, A. L., Paz, A. R., Aragao, L., Mu, Q., Malhi, Y., Collischonn, W., Rocha, H. R. & Running, S. W. 2013. Assessment of the MODIS global evapotranspiration algorithm using eddy covariance measurements and hydrological modelling in the Rio Grande basin. *Hydrological Sciences Journal-Journal Des Sciences Hydrologiques,* 58**,** 1658-1676.

Salati, E., Dall'olio, A., Matsui, E. & Gat, J. R. 1979. Recycling of water in the Amazon basin: an isotopic study. *Water Resources Research,* 15**,** 1250-1258.

Salati, E. & Vose, P. B. 1984. Amazon Basin: A System in Equilibrium. *Science,* 225**,** 129-138.

Saleska, S., Da Rocha, H., Huete, A., Nobre, A., Artaxo, P. & Shimabukuro, Y. 2013. LBA-ECO CD-32 Flux Tower Network Data Compilation, Brazilian Amazon: 1999−2006. Oak Ridge, Tennessee, USA: Oak Ridge National Laboratory Distributed Active Archive Center.

Schlesinger, W. H. & Jasechko, S. 2014. Transpiration in the global water cycle. *Agricultural and Forest Meteorology,* 189-190**,** 115-117.

Schwalm, C. R., Huntinzger, D. N., Michalak, A. M., Fisher, J. B., Kimball, J. S., Mueller, B., Zhang, K. & Zhang, Y. 2013. Sensitivity of inferred climate model skill to evaluation decisions: a case study using CMIP5 evapotranspiration. *Environmental Research Letters,* 8**,** 024028.

Seyler, F., Muller, F., Cochonneau, G., Guimarães, L. & Guyot, J. L. 2009. Watershed delineation for the Amazon sub-basin system using GTOPO30 DEM and a drainage network extracted from JERS SAR images. *Hydrological Processes,* 23**,** 3173-3185.

Shi, M., Liu, J., Worden, J. R., Bloom, A. A., Wong, S. & Fu, R. 2019. The 2005 Amazon Drought Legacy Effect Delayed the 2006 Wet Season Onset. *Geophysical Research Letters,* 46**,** 9082-9090.

Silvério, D. V., Brando, P. M., Macedo, M. N., Beck, P. S., Bustamante, M. & Coe, M. T. 2015. Agricultural expansion dominates climate changes in southeastern Amazonia: the overlooked non-GHG forcing. *Environmental Research Letters,* 10**,** 104015.

Skinner, C. B., Poulsen, C. J., Chadwick, R., Diffenbaugh, N. S. & Fiorella, R. P. 2017. The Role of Plant CO_2 Physiological Forcing in Shaping Future Daily-Scale Precipitation. *Journal of Climate,* 30**,** 2319-2340.

Sörensson, A. A. & Ruscica, R. C. 2018. Intercomparison and Uncertainty Assessment of Nine Evapotranspiration Estimates Over South America. *Water Resources Research,* 54**,** 2891-2908.

Spracklen, D. V., Arnold, S. R. & Taylor, C. M. 2012. Observations of increased tropical rainfall preceded by air passage over forests. *Nature,* 489**,** 282-285.

Spracklen, D. V., Baker, J. C. A., Garcia-Carreras, L. & Marsham, J. 2018. The Effects of Tropical Vegetation On Rainfall. *Annual Review of Environment and Resources,* 43**,** 14.1–14.26.

Sun, L., Baker, J. C. A., Gloor, E., Spracklen, D., Boesch, H., Somkuti, P., Maeda, E. & Buermann, W. 2019. Seasonal and Inter-annual Variation of Evapotranspiration in Amazonia Based on Precipitation, River Discharge and Gravity Anomaly Data. *Frontiers in Earth Science,* 7**,** 1–9.

Swann, A. L. S. & Koven, C. D. 2017. A Direct Estimate of the Seasonal Cycle of Evapotranspiration over the Amazon Basin. *Journal of Hydrometeorology,* 18**,** 2173-2185.

Taylor, K. E., Stouffer, R. J. & Meehl, G. A. 2012. An Overview of CMIP5 and the Experiment Design. *Bulletin of the American Meteorological Society,* 93**,** 485-498.

Teuling, A. J. 2018. A Forest Evapotranspiration Paradox Investigated Using Lysimeter Data. 17**,** 1–7.

Timpe, K. & Kaplan, D. 2017. The changing hydrology of a dammed Amazon. *Science Advances,* 3**,** e1700611.

Van Der Ent, R. J., Savenije, H. H., Schaefli, B. & Steele-Dunne, S. C. 2010. Origin and fate of atmospheric moisture over continents. *Water Resources Research,* 46**,** 1-12.

Victoria, R. L., Martinelli, L. A., Jefferson, M. & Jeffrey, R. 1991. Mechanisms of Water Recycling in the Amazon Basin: Isotopic Insights. *Ambio,* 20**,** 384-387.

Von Randow, C., Manzi, A. O., Kruijt, B., De Oliveira, P. J., Zanchi, F. B., Silva, R. L., Hodnett, M. G., Gash, J. H. C., Elbers, J. A., Waterloo, M. J., Cardoso, F. L. & Kabat, P. 2004. Comparative measurements and seasonal variations in energy and carbon exchange over forest and pasture in South West Amazonia. *Theoretical and Applied Climatology,* 78**,** 5-26.

Wang, K. & Dickinson, R. E. 2012. A review of global terrestrial evapotranspiration: Observation, modeling, climatology, and climatic variability. *Reviews of Geophysics,* 50.

Watkins, M. M., Wiese, D. N., Yuan, D.-N., Boening, C. & Landerer, F. W. 2015. Improved methods for observing Earth's time variable mass distribution with GRACE using spherical cap mascons. *Journal of Geophysical Research: Solid Earth,* 120**,** 2648-2671.

Wei, Z., Yoshimura, K., Wang, L., Miralles, D. G., Jasechko, S. & Lee, X. 2017. Revisiting the contribution of transpiration to global terrestrial evapotranspiration. *Geophysical Research Letters,* 44**,** 2792-2801.

Werth, D. & Avissar, R. 2004. The Regional Evapotranspiration of the Amazon. *Journal of Hydrometeorology,* 5**,** 100-109.

Wiese, D., Yuan, D., Boening, C., Landerer, F. & Watkins, M. 2018. JPL GRACE Mascon Ocean, Ice, and Hydrology Equivalent Water Height Release 06 Coastal Resolution Improvement (CRI) Filtered Version 1.0. *In:* TELLUS, N. J. P. L. (ed.). NASA Physical Oceanography DAAC.

Wiese, D. N., Landerer, F. W. & Watkins, M. M. 2016. Quantifying and reducing leakage errors in the JPL RL05M GRACE mascon solution. *Water Resources Research,* 52**,** 7490-7502.

Wilson, K., Goldstein, A., Falge, E., Aubinet, M., Baldocchi, D., Berbigier, P., Bernhofer, C., Ceulemans, R., Dolman, H., Field, C., Grelle, A., Ibrom, A., Law, B. E., Kowalski, A., Meyers, T., Moncrieff, J., Monson, R., Oechel, W., Tenhunen, J., Valentini, R. & Verma, S. 2002. Energy balance closure at FLUXNET sites. *Agricultural and Forest Meteorology,* 113**,** 223-243.

Wright, J. S., Fu, R., Worden, J. R., Chakraborty, S., Clinton, N. E., Risi, C., Sun, Y. & Yin, L. 2017. Rainforest-initiated wet season onset over the southern Amazon. *Proceedings of the National Academy of Sciences,* 114**,** 8481-8486.

Yin, L., Fu, R., Shevliakova, E. & Dickinson, R. E. 2013. How well can CMIP5 simulate precipitation and its controlling processes over tropical South America? *Climate Dynamics,* 41**,** 3127-3143.

Zemp, D., Schleussner, C.-F., Barbosa, H., Van Der Ent, R., Donges, J. F., Heinke, J., Sampaio, G. & Rammig, A. 2014. On the importance of cascading moisture recycling in South America. *Atmospheric Chemistry and Physics,* 14**,** 13337-13359.

Zemp, D. C., Schleussner, C.-F., Barbosa, H. M. J. & Rammig, A. 2017a. Deforestation effects on Amazon forest resilience. *Geophysical Research Letters,* 44**,** 6182-6190.

Zemp, D. C., Schleussner, C.-F., Barbosa, H. M. J., Hirota, M., Montade, V., Sampaio, G., Staal, A., Wang-Erlandsson, L. & Rammig, A. 2017b. Self-amplified Amazon forest loss due to vegetation-atmosphere feedbacks. *Nature Communications,* 8**,** 1-10.

Zeng, Z., Piao, S., Lin, X., Yin, G., Peng, S., Ciais, P. & Myneni, R. B. 2012. Global evapotranspiration over the past three decades: estimation based on the water balance equation combined with empirical models. *Environmental Research Letters,* 7**,** 014026.

Zhang, K., Kimball, J. S., Nemani, R. R. & Running, S. W. 2010. A continuous satellite-derived global record of land surface evapotranspiration from 1983 to 2006. *Water Resources Research,* 46**,** 21.

Zhang, K., Kimball, J. S., Nemani, R. R., Running, S. W., Hong, Y., Gourley, J. J. & Yu, Z. 2015a. Vegetation Greening and Climate Change Promote Multidecadal Rises of Global Land Evapotranspiration. *Scientific Reports.* The Author(s).

Zhang, K., Almeida Castanho, A. D., Galbraith, D. R., Moghim, S., Levine, N. M., Bras, R. L., Coe, M. T., Costa, M. H.,
    Malhi, Y. & Longo, M. 2015b. The fate of Amazonian ecosystems over the coming century arising from changes in
    climate, atmospheric CO_2, and land use. *Global Change Biology.*
900 Zhang, K., Kimball, J. S. & Running, S. W. 2016a. A review of remote sensing based actual evapotranspiration estimation.
    WIREs Water, 3**,** 834-853.
Zhang, L., Dawes, W. R. & Walker, G. R. 2001. Response of mean annual evapotranspiration to vegetation changes at
    catchment scale. *Water Resources Research,* 37**,** 701-708.
Zhang, Y., Peña-Arancibia, J. L., Mcvicar, T. R., Chiew, F. H. S., Vaze, J., Liu, C., Lu, X., Zheng, H., Wang, Y., Liu, Y. Y.,
905 Miralles, D. G. & Pan, M. 2016b. Multi-decadal trends in global terrestrial evapotranspiration and its components.
    Scientific Reports, 6**,** 19124.